ANALYSIS OF PILE BENDING IN THE SEISMIC ENVIRONMENT OF THE PUGET SOUND REGION

by

Sunirmal Banerjee

Washington State Transportation Center
Department of Civil Engineering
University of Washington
Seattle, Washington

Phase I Research Report: Agreement Y-2811, Task 26

Prepared for

Washington State Transportation Commission
Department of Transportation and
in cooperation with Concrete Technology Corporation

April 1985

TABLE OF CONTENTS

LIST OF TABLES

LIST OF FIGURES

I. INTRODUCTION

Damage to pile-supported structures in severe earthquake has been reported in the literature (Youd and Hoose, 1976; Kachadoorian, 1968; Fukuoka, 1966; Hideaki et al., 1976; Elliot and Nagai, 1973; and many others). In fact, it seems that pile failures of some form or other have necessarily been one of the outcomes of most major earthquakes. Failure by loss of bond at the connection of the pile to the superstructure, buckling of walls in steel pipe piles are some of the many ways these failures have been manifested. Furthermore, in many cases, liquifaction of upper weak soils has resulted in significant distortions and damage to pile foundations.

The high likelihood of pile failures and the potential for damage to critical structures induced by such failures have aroused considerable interest in recent years in the development of pertinent knowledge in the subject of soil-structure interaction under seismic loading (Lysmer et al., 1975; Novak, 1974; Roesset et al., 1976; Berger et al., 1977; Gazetas et al., 1984; Scott et al., 1982; and many others). Notwithstanding the extensive research efforts expended, the performance of piles is far from being fully understood and serious questions do remain unanswered. But what is particularly disturbing is that, citing this lack of knowledge as a basis, some regulations have already been proposed which virtually prohibit the use of prestressed concrete piles in critical structures in regions of high seismicity (ATC 3-06, 1978). Restrictions of this sort may have developed from the extrapolation of the results of one or two analytical studies of limited scope and extreme conditions, for example, the pile bending analyses performed by Margason and Holloway (1977).

In order to examine the question of whether prestressed concrete piles are unsuitable for "ATC category D" structures as determined during the industry review of ATC 3-06, a joint University-Industry co-operative experimental research was recently performed at the University of Washington. The experimental research involved investigation of the flexural capacity of prestressed concrete piles under cyclic loading conditions (Stanton et al., 1984). As a follow up, the present study was undertaken to investigate the curvature demand on these piles by a severe Puget Sound earthquake. The principal objectives were to carry out theoretical pile-soil interaction analyses for single prestressed concrete piles embedded in two representative sites of the region, subjected to a reasonably severe earthquake, and to evaluate the results.

While this report focuses mainly on the presentation and discussion of the results of the soil-pile interaction analyses performed for the study, it also provides a brief discussion of the available approaches to such analyses in Section 2. Section 3 describes how input motions for the study were selected and specified. The site conditions chosen for the study and the results of the free-field analyses are presented in Section 4. Sections 5, 6 and 7 present the results of the main analyses, an evaluation of previous studies and the conclusions drawn from this study.

2. METHODS OF ANALYSIS

Numerous sophisticated analytical approaches have been proposed in the literature for soil-structure interaction problems. The detailed description and discussions of these approaches are available in several state-of-the-art reports on the topic (Yoshimi, 1977; Lysmer, 1978; Johnson, 1981). Basically, the current approaches to the soil-structure

interaction analysis can be divided into two categories -- complete or direct methods, and substructure methods.

The complete or direct methods attempt to solve the problem in a single step, employing models which include the combined soil structure system. In other words, this method usually requires a large finite element model which includes both the structure and part of the site. Special conditions can be applied to the edges of the model (e.g. transmitting boundaries) in order to reduce the size of the model or to eliminate reflection from the boundaries. Substructure methods, on the other hand, attempt to break the complex soil-structure interaction problem into three separate steps: determination of site response, computation of dynamic stiffnesses of the foundation and analyses of structural response. In this approach, the soil is treated as a continuum and the structure as a discretized model. The soil response is obtained first without the structure. The dynamic stiffnesses of the foundation soil can be computed by one of the following ways of treating the soil-structure interface: rigid boundary, flexible boundary, or flexible volume method, according to the number of degrees of freedom at which the soil and the structure interact. Then, using the properties obtained at the soil-structure interface, a lumped-mass model of the structure can be analysed with a loading which depends on the free-field motion.

The controversy over the suitability or preferability of each method seems to be never ending. The situation has been aggravated by comparative studies which claim to show superiority of one method over the other. Such claims are usually made without the writer having a clear understanding of how to apply both methods. It is possible to obtain sensible results with either method, when properly applied, and each has its advantages and disadvantages (Kausel and Roesset, 1974). Wight (1977)

has also pointed out the consequences of adopting either method from parametric analyses of twelve actual problems. His general conclusion was that the cost of calculations were about the same; the direct "finite element approach was computer-intensive, while the lumped mass approach was manpower-intensive." With regard to the judgment required for analysis, Wight mentions, "the finite element approach is relatively straightforward in implementation, and very little is required of the analyst. On the other hand, the lumped mass approach requires that the analyst to quantify the effect of layers on the springs and dashpots, determine an appropriate input excitation, and establish a radiation damping coefficient." Another important consequence of the modeling approach adopted was also noted by Wight. His analyses show that for surface or near surface structures the lumped-mass results are more conservative, while "for increasing depths of embedment, the finite element results often exceed the lumped-mass results." Considering the points discussed above along with the fact that more conservative results were obtained by Margason from the finite element analysis, a finite element approach was adopted for this study. The mathematical justification and the procedures of analysis are described in detail by Lysmer et al. (1975). These are not repeated here for the sake of brevity. It should, however, be remembered that the equivalent linear soil-structure interaction analysis based on the computer code "FLUSH," though well accepted in the profession, does not provide exact answers to physical problems. It is a two-dimensional finite element program, by which the three-dimensional responses of systems can be approximated. Furthermore, like all its equivalents which are currently available, this analysis suffers from uncertainties arising from lack of full confirmation

with measured response. However, limited comparison of FLUSH-based predictions with the observed response of Humboldt Bay Nuclear Power Plant to shaking by the Ferndale Earthquake of June 1975 has shown good agreement (Valera et al., 1977).

3. SPECIFICATION OF INPUT MOTION

One of the most significant decisions to be made before any meaningful results can be obtained from a soil-structure interaction analysis is the choice of the earthquake motion to be specified for the analysis. This also involves making decisions about the type of wave field and location of the control motion, i.e., the control point. Doubtless, a considerable degree of uncertainty exists in this very first step. But specification of a reasonable control motion can be made on the basis of sound judgment and assessment of the seismic risk in the Puget Sound region.

Review of Seismicity of Puget Sound Region: Low to moderate intensity earthquakes have been relatively frequent in the Puget Sound region. Two of the more severe historic earthquake events in the region were recorded on April 13, 1949 in Olympia (Richter magnitude 7.1, maximum intensity, MM VIII) and on April 29, 1965 in Seattle (Richter magnitude 6.5, maximum intensity, MM Low VIII). Seismic history of the region has been accumulated and studied by several investigators (Rasmussen, 1976; Rasmussen et al., 1974; Perkins et al., 1980). These studies indicate that the dominant tectonic activity in this region has been associated mainly with the subcrustal interaction along the boundary of the North American plate. Although the subduction zone at the confluence of the Juan de Fuca plate and the North American plate is possibly the source of most of the tectonic events in the region, adequate information about the

distribution of the tectonic events along this subduction zone is not available.

The larger earthquakes which have occurred in this region were of deep origin (approximately 70 km and 57 km deep in the 1949 and 1965 events respectively). And, unlike the California earthquakes, these earthquakes have not been accompanied by or concentrated along surface fault rupture. Therefore, the so called "deterministic" approach of establishing design events from empirical correlations between length of fault rupture, distance to fault and the maximum bedrock acceleration (Seed et al., 1968) applicable to the Western United States does not apply to this region. Although Patwardhan and others (Idriss, 1978) have proposed several correlations applicable for subduction zone activity, it did not seem meaningful for this study to establish the parameters of a very large earthquake from these correlations. A recent probabilistic study (Perkins et al., 1980), on the other hand, has concluded that the maximum bedrock acceleration for a 500-year return period in the Puget Sound region is estimated to range from 0.10 g to 0.30 g. The Olympia event certainly fits in this range and if a direct use of the recorded motion is made, the other characteristics of a large regional earthquake will be preserved. The estimated range, of course, does not account for the variation in local soil conditions which, in many cases, have great influence on the ground surface acceleration. Hawkins and Crosson (1975) have also pointed out that a quake of the size of the Olympia event may recur every 100 to 200 years anywhere in the Puget Sound region. In other words, considering the great depth of focus of the large quakes, they further suggest that there is equal likelihood of an Olympia event being recorded in Seattle or Tacoma within these return periods. So, for this

study it was decided to work with the motion recorded in the Olympia Highway Test Lab in 1949.

Wave Content of the Control Motion: Although actual recorded earthquake motions may include a train of body waves and surface waves, at present it is not practical to take into account all of these types of wave fields in a seismic analysis. Fortunately, however, careful investigations (Seed and Lysmer, 1981; Chen et al., 1981) have revealed that the components of surface waves with frequencies higher than 1 Hz decay rapidly within a few hundred feet of the source. It has also been known previously that the effects of Rayleigh waves become relatively insignificant within a distance of five times the focal depth (Perkeris and Lifson, 1957). From their studies, Chen et al. (1981) concluded that the customary assumption of vertically propagating shear waves practically is sufficient in most seismic environment and is likely to produce conservative results. For this study, therefore, only vertically propagating shear waves are considered.

Location of the Control Point: For the soil-structure interaction analysis, a control point must be chosen where the input motion is to be specified. Since earthquake motions at the ground surface are dependent upon the subsurface conditions which vary from site to site, simply specifying a ground surface motion obtained from one site as a control motion at another site is not appropriate and results in incompatible motions at depths. The most reasonable alternative is to apply the control motion at a hypothetical rock outcrop and to compute a compatible motion at the base of the soil profile of interest. This base motion can then be specified as the control motion for the analysis.

Deconvolution Analysis: The hypothetical rock outcrop motion mentioned earlier is obtained from a deconvolution analysis, i.e., an inverse analysis which computes the compatible base motion and the rock outcrop motion which must have yielded the ground surface motion at the recording site. In this study, the April 13, 1949 Olympia event, which is the largest historical earthquake felt in this region, was chosen so that the particular nature of a Puget Sound earthquake can be preserved. This earthquake was recorded at the Highway Test Laboratory station in Olympia approximately 16 km away from the epicenter. The acceleration-time history used in the analysis is the N86E component record of 30 second duration and having a peak acceleration of 0.28 g. This record was digitized, processed and baseline corrected at California Institute of Technology (Hudson et al. 1971-1975, Vol. IIB).

This accelerogram (shown in Fig. 1) and the computer program SHAKE (Schaabel et al. 1972) were used to perform the deconvolution analysis. The soil profile (at the Test Lab site) used in the analysis is shown in Table 1. The in-situ shear wave velocity and penetration data at this site was obtained from a previous report (Shannon and Wilson and Agabian Associates, 1980). The strain-dependent of dynamic soil properties, shear modulus and damping ratio values used for the analysis are shown on Figs. 2 and 3 respectively (Seed and Idriss, 1970). The material curves for damping ratio (for all the analyses in this study) was further adjusted to account for the effects of the degree of saturation and the effective overburden pressures (Schnabel, 1973).

It is appropriate to note a few of the approximations involved in the analysis. First of all, during the course of the field investigations at the site, the depth to bedrock was not established, but is known to be very deep and of the order of 1,000 or more feet. The existence of rock-

like materials is, however, revealed from the in-situ shear wave velocity measurements. At 420 feet below ground, there was a sharp rise in the measured value of the shear wave velocity (to about 3,200 ft./sec.). In the deconvolution analysis, the depth to bedrock was chosen to be 420 ft. Secondly, the results of deconvolution analysis are usually affected by the cut-off frequency. A sensitivity study was performed to determine this effect. Fig. 4, which plots the peak accelerations at various depths for analyses for 20 Hz and 25 Hz cut-off frequencies, indicates that the differences are relatively minor. Accordingly, a cut-off frequency of 20 Hz was selected in all subsequent analyses in order to reduce the cost of analysis. Also, the effects of the duration of quiet zone in the acceleration-time history and of the thickness of the soil layers were also checked systematically to assure that reasonably accurate results are obtained.

The acceleration-time history at hypothetical outcropping rock layer at a depth of 250 ft. was obtained from the deconvolution analysis at the Olympia site. The principal reason for choosing 250 ft. depth for the outcropping layer is that the field investigations performed at the two representative sites chosen (for the soil-structure interaction analyses) were not extended to bedrock, nor to a rock-like layer. But this seemingly arbitrary choice of the bedrock level, fortunately, does not affect the structural response as long as the base of the soil model is at a large distance away from the base of the structure (Hwang, 1974). The computed rock outcrop motion is shown in Fig. 5.

4. SITE CONDITIONS AND FREE-FIELD ANALYSES

For the soil-pile interaction study, two representative soil profiles were carefully chosen from two local projects: 1) West Seattle Freeway

Bridge Replacement Project in Seattle and 2) Central Waste Water Treatment plant project in Tacoma. The geotechnical engineering evaluation studies for both of the projects were performed by Shannon and Wilson, Inc. (Shannon and Wilson, 1977 and 1980). The site conditions at these projects will be referred to hereafter as "West Seattle site" and "Tacoma site" respectively.

West Seattle Site: At the West Seattle Bridge project location, the subsurface condition generally consist of varying thicknesses of alluvial sandy deposit overlying glacial soils. The cross-section for analysis was modeled as a 100-ft thick alluvial deposit underlain by glacial deposit extending up to bedrock level at 250 ft. below the ground surface. In order to account for the uncertainty in the soil properties, it was decided that the range of soil properties obtained from in-situ shear wave velocity measurements, standard penetration tests and laboratory tests should be covered. Therefore, six profiles were characterized by varying the soil properties of various layers. These profiles (shown in Tables 2 to 7) were then analyzed using the program SHAKE to conduct the free-field analyses, i.e. analyses of the ground response in the absence of any structure. The strain-dependent modulus reduction curves used for the West Seattle soils are shown in Fig. 6 (from Shannon and Wilson, 1980). The results of the SHAKE analyses are illustrated in Fig. 7. It can be observed that the maximum acceleration vs. depth curves approximately fall into two groups. The results from the analysis of the third and fourth profiles represent the first group, and those from the second, fifth and sixth profiles represent the second group; the results from the first profile lie somewhat in between those of the two groups. It is worth mentioning that in the first group of profiles that modulus values

represent the lower boundary of the observed range in the alluvial deposit and the average values in the glacial deposit. The second group of profiles is characterized by the observed upper bound modulus values in both alluvial and glacial soils.

On the basis of this preliminary analysis, the fourth and sixth West Seattle profiles were selected for the subsequent soil-profile interaction analyses at this site. The base motions at 250-ft. level were obtained for these profiles from the prescribed outcrop motion. These base motions, which were later applied at the base of the finite element model, are shown in Figs. 8 and 9 for the fourth and the sixth profile respectively.

Tacoma Site: In the same manner, three soil profiles as shown in Tables 8 to 10 were established for SHAKE analyses at the Tacoma site. Since the strain-dependent soil properties were not investigated for this project, the empirical curves shown in Figs. 2 and 3 (Seed and Idriss, 1970) used to account for the strain-dependent behavior of the soils at this site. The damping ratio curves were adjusted for degree of saturation and overburden pressure effects. The results of this analysis are shown in Fig. 10. It can be noted that the results are virtually the same for the first and the third profile. Therefore, the second and the third profile from this site were selected for the soil-pile interaction analysis. The base motions at 250-ft. level obtained from the analyses are shown in Figs. 11 and 12 for the second and the third profile, respectively.

5. SOIL-PILE INTERACTION ANALYSES

The soil-pile interaction analyses were performed by the direct method based on the finite element program FLUSH. This program is a

variation from its predecessor LUSH (which is the basic two-dimensional model used by Margason) in that it is far more efficient and capable of approximately simulating three-dimensional effects by the use of viscous boundaries in the third dimension.

The finite element meshes used for the two sites are shown in Fig. 13. Considering the symmetry of the problem, only half of the soil-structure system was analyzed. The pile was represented by several beam elements. The translational nodes along the left edge were kept fixed in the vertical direction to satisfy symmetry requirements. On the right edge of the model, transmitting boundary conditions were imposed at all the nodes so that it is not necessary to have an extensive mesh in the horizontal direction. In order to insure that reasonable results were in fact obtained, the accelerations at the nodes on the transmitting boundary were compared to those obtained from the free-field analyses using SHAKE.

In all the analyses, the results compared well. A check of the sensitivity of results to the element sizes was performed by comparing the results obtained from the meshes shown in Fig. 13 and several of its variations. Finally, for this study only three sizes of octagonal piles, 24", 18" and 14", were used. The properties of these piles are shown in Table 11. The effect of a pile cap and the applied vertical load was also simulated by attaching a concentrated mass to the translational node at the top of the pile.

Results and Discussion

West Seattle Site: Fig. 14 shows the maximum induced curvature, K(=M/EI) on a 14 in. pile along the length of the pile for the fourth and sixth profile at this site. A strong influence of the soil properties on the induced curvature is revealed by this figure. In other words, the softer

the soil deposit, the higher are the values of the induced curvature. It is important to remember here that the peak free-field ground accelerations were computed as 0.24 g and 0.35 g for the fourth and the sixth profile (Fig. 7) respectively for the same outcrop motion at 250 ft. depth. Therefore, higher value of peak ground acceleration does not necesarily mean higher curvatures on the pile.

Inspection of Fig. 14 also reveals that there are two peaks in the plot of curvature with depth. The upper peak is a result of the concentrated mass placed at the top of the pile. This effect is more pronounced in Fig. 15, which shows the results of varying the concentrated mass in the upper 20 ft; the curvatures below 20 ft. depth remain the same for both cases. The second peak in Fig. 14 is due to the existence of the interface between softer and stiffer soils. Particularly for the fourth profile, it is not surprising that a marked peak is noticeable at the interface since the change in the modulus of soils on both sides of the interface is quite sharp.

The effect of pile size on the induced curvatures is illustrated by Figs. 16 and 17. Excluding the effect of the concentrated mass at the top of the pile, the induced curvature tends to reduce with increasing pile diameter, especially at the alluvium-glacial till interface. Figs. 18, 19 and 20 show the results for the different pile sizes with the top of the piles restrained from rotation. Fixing the piles from rotating at the top end results in a substantially high induced curvature at the connection with the cap; the curvatures below 20 ft. depth remain nearly the same as the free end case. These results show that the pile-pile cap connection is a critical point where sharply high curvatures can be expected in all practical situations. Finally, the effect of a higher base motion was investigated by applying a scaling factor of 1.2 to the base motion of the

fourth profile (Fig. 8). The curvatures induced in this case are shown in Fig. 21, and can be compared with their counterparts on Fig. 18 to observe the effect of a higher input motion.

Some of the other pertinent results are also shown here for the purpose of illustration. Figs. 22 and 23 are the acceleration-time history plots (for the fourth profile) at the top of the 14" pile and at the ground surface in the free-field respectively. Figs. 24 and 25 show the variation of spectral accelerations with depth along the pile and in the free-field respectively comparison of spectral accelerations at the 100 ft. depth on 14" and 24" piles and in the free-field is made on Fig. 26. This shows that there is no significant difference in the spectral acceleration values. Also, the acceleration spectra plotted in Fig. 27 show the effect of increasing concentrated mass at the top of the pile. Fig. 28 shows the effect of the soil profile on the velocity spectra by comparing the results for the fourth and sixth profile.

Tacoma Site. Fig. 29 illustrates the behavior of a 14 in. pile embedded in the second and the third profile at the Tacoma site. It can be noted that there are several peaks in the maximum induced curvature vs. depth plot for this particular site. Generally, the peaks occur at the interfaces of soil layers where changes in modulus values are significant. In addition, the peaks also occur at the clay-sand interfaces at depths of 18 ft. and 35 ft. because of the difference in the strain-dependent behavior of these soils. However, no such peak does develop at the depth of 18 ft. in the second profile; this may be the result of an increase in the low-strain modulus in the clay layer. It should also be noted that the existence of a layer with high modulus sandwiched between two softer layers could result in high pile curvature.

The conclusions about the effect of pile size derived from the West Seattle site results are borne out by the results at this site. Fig. 30 shows the effects of pile sizes on the induced curvature. The decrease in induced curvature with increasing pile size is particularly significant in this case in the upper portion of the piles where breaks in curvature develop.

The plots of acceleration spectra at various depths on the pile and in the free-field for the third profile at the Tacoma site are illustrated in Figs. 31 and 32 respectively. Fig. 33 shows the effect of pile size on the acceleration spectra and a comparison with the free-field acceleration spectra. Figs. 34 and 35 show the comparison of acceleration and velocity spectra for the two profiles considered at this site. Finally, Figs. 36 and 37 are the plots of ground surface motions in the free-field for the second and third profile respectively and to compare with these, the motion at the top of the 14 in. pile embedded in the third profile is also included in Fig. 38.

6. EVALUATION OF PRIOR STUDIES

Approximate analyses of the theoretical performance of prestressed concrete piles in the seismic environment of the San Francisco Bay area were performed by Margason and Holloway (1977). This study was conducted as a part of the post-design analysis for a pile-supported multi-storied building project at Emeryville, California and the analysis was limited to 90-ft. long, 12-in. square prestressed concrete piles.

Two different computational approaches were used for performing the seismic pile bending analysis. These analysis approaches were based on lumped-mass (Idriss and Seed, 1970) and finite element (Lysmer at al., 1974) formulations proposed for seismic response analysis of soil deposits

and soil-structure interaction problems respectively. Unfortunately, in either case the pile motion was approximated by the motion of a one-dimensional column of the surrounding soil. In other words, neither of the adopted approaches accounted for the interaction effects between the pile and the surrounding soil. And, on the basis of the assumption that the pile motion is equal to and in phase with the soil, the computed curvatures of the soil column were, in fact, reported as the induced pile curvatures. It is obvious that computation of pile curvatures from soil displacements rather than from the induced bending moments on the pile can only give "worst case" predictions (Holloway, 1985) which, in general, means large positive errors in the predictions.

Hence, it was considered appropriate to reanalyse their problem with the computational approach used in the present study. Since the exact input parameters from the above-mentioned study were not available, it was decided to perform the present analysis on a 90-ft. long, 12-in. square prestressed concrete pile embedded in a soil profile representative of the Southern Pacific Railroad building site in San Francisco. The soil profile at this site is nearly identical in sequence and characteristics with that at the Emeryville site. It should be noted that no site-specific exploration was actually carried out for obtaining the dynamic characteristics of the soils at Emeryville. These were estimated from the static strength and index properties (Seed and Idriss, 1970). The choice of the San Francisco site, on the other hand, was based on the fact that the actual soil and subsurface data for this site were available from literature sources (Idriss and Seed, 1968). The data for this site are shown in Table 12. However, the earthquake input motion parameters used for the present analysis were unchanged from those specified in the

previous study. The analysis was performed with the Taft N21E record of the 1952 Kern County earthquake. This accelerogram was scaled to yield an outcrop motion at 285 ft. with peak acceleration of 0.45 g and a predominant period of 0.42 second. This motion corresponds to an earthquake of magnitude 8-1/4 with an epicentral distance of 16 km.

At the San Francisco site, the free-field response was computed for the profile shown in Table 12. Fig. 39a), b), and c) show the computed base rock motion time history, variation of maximum ground acceleration with depth and the finite element model used for soil-pile interaction analyses. Fig. 40 shows the maximum induced curvatures on a 12-in. pile with both fixed and free rotational end conditions at the pile-cap connection. The same figure also shows the predictions of Margason and Holloway for comparison. The maximum induced curvature of the order of 2.2×10^{-4} inches $^{-1}$ obtained for the San Francisco site is certainly consistent with the results for the West Seattle and Tacoma sites. The differences in the predictions from this study and from the previous analyses performed by Margason and Holloway is attributable to the less accurate analysis procedures available at that time, as has been pointed out earlier.

7. SUMMARY AND CONCLUSIONS

This analytical study was undertaken to investigate the theoretical performance of concrete piles in the seismic environment of the Puget Sound region, and to evaluate the consistency of these results with those of some prior investigations. It must be mentioned that the intent of study was neither to exhaustively cover all possible soil profile variations of this region nor to examine the effect of all likely earthquake events. A limited but realistic assessment of the problem was

made in this study by selecting a severe local earthquake loading and two soil profiles representative of this area. While analyses of the type presented here are approximate in nature, they provide the designer with a reasonable estimate of the potential for damage, and can be employed economically when questions arise as to the possible suitability of a given pile in a given soil condition. Based on these analyses several general conclusions can be drawn:

1. The maximum induced curvatures in piles are signficantly affected by the behavior of the soil deposits and become especially critical at the interface between layers with significantly different modulus values.
2. For the same soil deposits, the maximum induced curvatures reduce with increasing pile size.
3. The effect of axial load and fixity at the pile to pile-cap connection can be most severe in causing curvature demand, but this effect remains concentrated in the upper portion of the pile.
4. The severity of the earthquake may have a direct relationship with the maximum induced curvature. This severity is not synonymous with higher peak ground acceleration. Higher peak ground acceleration does not necessarily mean that the induced curvature in piles are higher.

While previous analyses predicted that curvatures of the order of 6×10^{-4} inches $^{-1}$ may be induced in piles embedded in soil profiles typical of San Francisco Bay conditions, an analysis of a nearly identical problem performed for this study suggests that such high curvatures may not possibly be induced even for the extreme conditions considered. This

deviation is primarily due to the less accurate analysis approaches employed in the previous study. The maximum curvature for the 12-in. piles embedded in the San Francisco site was predicted to be about 2.2 x 10^{-4} in. in this study. For piles embedded in the Puget Sound region soil profiles, analyses show that even for a fairly severe earthquake and the relatively poor soil conditions, the maximum induced curvatures range from 0.1 x 10^{-4} to 1.2 x 10^{-4} inches $^{-1}$. Previous experimental studies have shown that curvatures of such magnitude can be easily withstood by prestressed concrete piles (Xuekang et al., 1984; Stanton et al., 1984). Finally, for extremely poor soil conditions, and very severe dynamic loading, the alternative of replacement or stabilization of weaker soils should be weighed economically and technically against designs that employ very high curvature-capacity piles. Any blanket restriction of one pile type or the other without site-specific analyses is not warranted.

ACKNOWLEDGEMENTS

The work reported was partially supported by a corporate-affiliate gift from Concrete Technology Corporation. The help from Paul Grant of Shannon and Wilson, Inc. in locating the soil and subsurface data is gratefully acknowledged. Finally, computational assistance from Mr. V. Vitayasupakorn, a graduate student in the Civil Engineering Department, is also appreciated.

REFERENCES

1. "Tentative Provisions for the Development of Seismic Regulations for Buildings," prepared by Applied Technology Council Associated with SEOAC, ATC Publication ATC 3-06, June 1978.

2. Berger, E. et al. (1977), "Simplified Method for Evaluating Soil-Pile-Structure Interaction Effects," Proceedings of 9th Offshore Technology Conference, Houston, TX, OTC Paper No. 1954.

3. Chen, J. C. et al. (1981), "Analysis of Local Variations in Free Field Seismic Ground Motion," Report No. UCB/EERC-81/03, U.C., Berkeley, January.

4. Elliot, A. L. and Nagai, I. (1973), "Earthquake Damage to Freeway Bridges," San Fernando 1971 Earthquake Study by NOAA, Vol. II, U.S. Department of Commerce.

5. Fukuoka, M. (1966), "Damage to Civil Engineering Structure," Soils and Foundations, JSCE, Vol. 6, No. 2, March.

6. Gazetas, G. and Dobry, R. (1984), "Horizontal Response of Piles in Layered Soils," Journal of Geotechnical Division, ASCE, Vol. 110, No. 1, January.

7. Hawkins, N. M. and Crosson, R. S. (1975), "Causes, Characteristics and Effects of Puget Sound Earthquakes," Proceedings of the U.S. National Conference on Earthquake Engineering, Ann Arbor, EERI, June.

8. Hideaki, K. et al. (1980), "Damage of Reinforced Precast Pile During the Miyagi Kenoki Earthquake of June 12th, 1972," Seventh World Conference on Earthquake Engineering, Vol. 9, Istanbul.

9. Hudson, D. E. et al. (1971-1975), "Strong-Motion Earthquake Accelerograms, Digitized and Plotted Data," California Institute of Technology, Earthquake Engineering Research Lab., Pasadena, Vol. IIB.

10. Hwang, R. (1974), "Seismic Response of Embedded Strutures," Ph.D. Dissertation submitted in partial fulfillment for degree of Doctor of Philosophy, Department of Civil Engineering, U.C., Berkeley, June.

11. Holloway, D. M. (1985), Personal Communications.

12. Idriss, I. M. (1978), "Characteristics of Earthquake Ground Motions," Proc. ASCE Speciality Conference on Earthquake Engineering and Soil Dynamics, Vol. III, Pasadena, CA.

13. Idriss, I. M. and Seed, H. B., (1970), "Seismic Response of Soil Deposits," ASCE, SMFDIV, March.

14. Idriss, I. M. and Seed, H. B. (1968), "An Analysis of Ground Motions During the 1957 San Francisco Earthquake," Bulletin of Seismological Society of America, Vol. 58, No. 6, pp. 2013-2032, December.

15. Johnson, J. J. (1981), "Soil Structure Interaction: The Status of Current Analysis Methods and Research," Seismic Safety Margins Research Program, Lawrence Livermore Lab, NUREG/CR-1780, UCRL-53011, January.

16. Kachedoorian, R. (1968), "Effects of Earthquake of March 27th, 1974, On the Alaska Highway System," Geological Survey Professional Paper 545-C, U.S. Department of Interior, Washington, D.C.

17. Kausel, E. and Roesset, J. M. (1974), "Soil Structure Interaction for Nuclear Containment Structures," Proc. ASCE Power Div. Speciality Conference, Boulder, CO, August.

18. Lysmer, J. (1978), "Analytical Procedures in Soil Dynamics," Proc. ASCE Specialty Conference on Earthquake Engineering and Soil Dynamics, Vol. III, Pasadena, CA, June.

19. Lysmer, J., Udaka, T., Seed, H. B. and Hwang, R. (1974), "LUSH -- A Computer Program for Complex Response Analysis of Soil-Structure Systems," Report No. EERC 74-4, U.C., Berkeley, April.

20. Lysmer, J. et al. (1975), "FLUSH -- A Computer Program for Approximate 3-D Analysis of Soil-Structure Interaction Problems," Report No. EERC 75-30, U.C., Berkeley, November.

21. Margason, E. (1977), "Earthquake Effects on Embedded Pile Foundations," Paper presented at the Pile Talk Seminar, San Francisco, CA, March.

22. Margason, E., and Holloway, D. M. (1977), "Pile Bending During Earthquakes," 6th World Conference on Earthquake Engineering, New Delhi, India, January.

23. Novak, M. (1974), "Effect of Soil on Structural Response to Wind and Earthquake," Int. J. Earthquake Engineering and Structural Dynamics, Vol. 3, pp. 79-96.

24. Pekeris, C. C. and Lifson, H. (1957), "Motion of the Surface of a Uniform Elastic-Halfspace Produced by a Buried Pulse," J. Acoust. Soc. America 20, 1233.

25. Perkins, D. et al. (1980), "Probabilistic Estimates of Maximum Seismic Horizontal Ground Motion on Rock in the Pacific Northwest and the Adjacent Outer Continental Shelf," USGS, Open File Report No. 80-471.

26. Rasmussen, N. H. et al. (1974), "Earthquake Hazard Evaluation of the Puget Sound Region, Washington State," U.W. Department of Geophysics, Seattle.

27. Roesset, J. M. and Kausel, E. (1976), "Dynamic Soil Structure Interaction," 2nd Intl. Conf. on Numerical Methods in Geomechanics, ASCE, V.P.I., Blacksburg, VA.

28. Schnabel, P. B. et al. (1972), "SHAKE-A Computer Program for Earthquake Response Analysis of Horizontally Layered Sites," Report No. EERC 72-12, U.C., Berkeley, December.

29. Schnabel, P. B. (1973), "Effects of Local Geology and Distance From Source on Earthquake Ground Motions," Ph.D. Dissertation submitted in partial fulfillment of the degree of Doctor of Philosophy, Dept. of Civil Engineering, U.C., Berkeley, June.

30. Scott, R. F. et al. (1982), "Full Scale Dynamic Lateral Pile Tests," Proc. 14th Offshore Technology Conference, Houston, TX, OTC Paper No. 4203.

31. Seed, H. B., et al. (1968), "Characteristics of Rock Motions During Earthquakes," Report No. EERC 68-5, U.C., Berkeley, December.

32. Seed, H. B. and Idriss, I. M. (1970), "Soil Moduli and Damping Factors for Dynamic Response Analysis," Report No. EERC 70-10, U.C., Berkeley, December.

33. Seed, H. B. and Lysmer, J. (1981), "The Seismic Soil-Structure Interaction Problem for Nuclear Facilities," Soil Structure Interaction: The Status of Current Analysis Methods and Research, Seismic Safety Margins Research Program, Jonson, J. J. (3d.), NUREG/CR-1780, UCRL-53011, January.

34. Shannon and Wilson, Inc. (1977), "Foundation Explorations, Phase I, Central Waste Water Treatment Plant, Tacoma, WA, Summary Report to Consoer Townsend and Assoc., November.

35. Shannon and Wilson, Inc. (1980), "Geotechnical Engineering Studies, West Seattle Freeway Bridge Replacement, City of Seattle -- Main Span Substructure, Harbor Island Structure," Report to Andersen-Bjornstad-Kane-Jacobs, Inc., August.

36. Shannon and Wilson, Inc. and Agbabian Assoc. (1980), "Geotechnical and Strong Motion Earthquake Data from U.S. Accelerograph Stations -- Anchorage, AK; Seattle, WA; Olympia, WA; Portland, OR," NUREG/CR-0985, Vol. 4, Report to the U.S. Nuclear Regulatory Commission, September.

37. Stanton, et al. (1984). "Lateral Load Tests on Prestressed Piles," 8th World Conference on Earthquake Engineering, Vol. VI, EERI, San Francisco, July.

38. Valera, J. E. et al. (1977), "Seismic Soil-Structure Interaction Effects at Humbolt Bay Power Plant," Journal of Geotechnical Engineering Division, ASCE, Vol. 103, No. GT10, pp. 1143-1161, October.

39. Wight, L. H. (1977), "Soil-Structure Interaction in Nuclear Power Plants: A Comparison of Methods," 6th World Conference on Earthquake Engineering, New Delhi, India, January.

40. Xuekang, T. et al. (1984), "Prediction of the Response of Prestressed Concrete Piles to Seismic Loading," Bulgarian-American Seminar on Seismic Safety of Prefabricated Concrete Buildings, Bulgarian Academy of Sciences, National Committee for Earthquake Engineering, Sofia.

41. Yoshima, Y. et al. (1977), "Soil Dynamics and Its Application to Foundaton Engineering," Proc. 9th Intl. Conference on Soil Mechanics and Foundation Engineering, Vol. 2 and 3, Tokyo.

42. Youd, T. L. and Hoose, S. N. (1976), "Liquefaction During 1906 San Francisco Earthquake," Journal of Geotechnical Division, ASCE, Vol. 102, No. GT5, May.

TABLE 1. SOIL PROPERTIES AT OLYMPIA SITE

Depth, ft.	Soil Type (Mat. Curve)	Unit Weight pcf	Low Strain Shear wave velocity (at 10^{-4}%)fps
0 - 10 *	FILL (2)	100	500
10 - 25	SAND (2)	120	750
25 - 40	SAND (2)	120	860
40 - 75	CLAY (1)	120	1470
75 - 135	CLAY (1)	120	1670
135 - 200	SAND (2)	125	1350
200 - 300	SAND (2)	125	1530
300 - 420	SAND (2)	125	1880
420	BASE	135	3200

* Water Table at 10 feet.

TABLE 2. SOIL PROPERTIES AT W. SEATTLE SITE: 1st PROFILE

Depth, ft.	Soil Type (Mat. Curve)	Unit Weight pcf	Low Strain Shear Wave Velocity (at 10^{-4}%), fps
0 - 10 *	ALLUVIUM (2)	120	550
10 - 30	ALLUVIUM (2)	120	600
30 - 50	ALLUVIUM (2)	120	675
50 - 100	ALLUVIUM (2)	120	800
100 - 180	GLACIAL (1)	130	1800
180 - 250	GLACIAL (1)	130	2150
250	BASE	135	2500

* Water Table at 10 Feet.

TABLE 3. SOIL PROPERTIES AT W. SEATTLE SITE: 2nd PROFILE

Depth, ft.	Soil Type (Mat. Curve)	Unit Weight pcf	Low Strain Shear Wave Velocity (at 10^{-4}%), fps
0 - 10 *	ALLUVIUM (2)	120	550
10 - 30	ALLUVIUM (2)	120	750
30 - 50	ALLUVIUM (2)	120	1000
50 - 100	ALLUVIUM (2)	120	1150
100 - 140	GLACIAL (1)	130	1700
140 - 180	GLACIAL (1)	130	2000
180 - 250	GLACIAL (1)	130	2150
250	BASE	135	2500

* Water Table at 10 Feet.

TABLE 4. SOIL PROPERTIES AT W. SEATTLE SITE: 3rd PROFILE

Depth, ft.	Soil Type (Mat. Curve)	Unit Weight pcf	Low Strain Shear Wave Velocity (at 10^{-4}%), fps
0 - 10 *	ALLUVIUM (2)	120	300
10 - 30	ALLUVIUM (2)	120	400
30 - 50	ALLUVIUM (2)	120	450
50 - 100	ALLUVIUM (2)	120	500
100 - 140	GLACIAL (1)	130	1050
140 - 180	GLACIAL (1)	130	1200
180 - 250	GLACIAL (1)	130	1400
250	BASE	135	2500

* Water Table at 10 Feet.

TABLE 5. SOIL PROPERTIES AT W. SEATTLE SITE: 4th PROFILE

Depth, ft.	Soil Type (Mat. Curve)	Unit Weight pcf	Low Strain Shear Wave Velocity (at 10^{-4}%), fps
0 - 10 *	ALLUVIUM (2)	120	300
10 - 30	ALLUVIUM (2)	120	400
30 - 50	ALLUVIUM (2)	120	450
50 - 100	ALLUVIUM (2)	120	500
100 - 140	GLACIAL (1)	130	1600
140 - 180	GLACIAL (1)	130	1800
180 - 250	GLACIAL (1)	130	2000
250	BASE	135	2500

* Water Table at 10 Feet.

TABLE 6. SOIL PROPERTIES AT W. SEATTLE SITE: 5th PROFILE

Depth, ft.	Soil Type (Mat. Curve)	Unit Weight pcf	Low Strain Shear Wave Velocity (at 10^{-4}%), fps
0 - 10 *	ALLUVIUM (2)	120	700
10 - 30	ALLUVIUM (2)	120	800
30 - 50	ALLUVIUM (2)	120	950
50 - 100	ALLUVIUM (2)	120	1100
100 - 140	GLACIAL (1)	130	1600
140 - 180	GLACIAL (1)	130	1800
180 - 250	GLACIAL (1)	130	2000
250	BASE	135	2500

* Water Table at 10 Feet.

TABLE 7. SOIL PROPERTIES AT W. SEATTLE SITE: 6th PROFILE

Depth, ft.	Soil Type (Mat. Curve)	Unit Weight pcf	Low Strain Shear Wave Velocity (at 10^{-4}%), fps
0 - 10 *	ALLUVIUM (2)	120	700
10 - 30	ALLUVIUM (2)	120	800
30 - 50	ALLUVIUM (2)	120	950
50 - 100	ALLUVIUM (2)	120	1100
100 - 140	GLACIAL (1)	130	2000
140 - 180	GLACIAL (1)	130	2200
180 - 250	GLACIAL (1)	130	2500
250	BASE	135	2500

* Water Table at 10 Feet.

TABLE 8. SOIL PROPERTIES AT TACOMA SITE: 1st PROFILE

Depth, ft.	Soil Type (Mat. Curve)	Unit Weight pcf	Low Strain Shear Wave Velocity (at 10^{-4}%), fps
0 - 10 *	FILL (2)	120	400
10 - 18	SAND (2)	120	400
18 - 35	CLAY (1)	120	400
35 - 60	SAND (2)	120	470
60 - 75	SAND (2)	120	600
75 - 117	SAND (2)	120	850
117 - 140	SAND (2)	120	1000
140 - 180	SAND (2)	130	1200
180 - 250	SAND (2)	130	1500
250	BASE	135	2500

* Water Table at 10 Feet.

TABLE 9. SOIL PROPERTIES AT TACOMA SITE: 2nd PROFILE

Depth, ft.	Soil Type (Mat. Curve)	Unit Weight pcf	Low Strain Shear Wave Velocity (at 10^{-4}%), fps
0 - 10 *	FILL (2)	120	400
10 - 18	SAND (2)	120	400
18 - 35	CLAY (1)	120	550
35 - 60	SAND (2)	120	900
60 - 75	SAND (2)	120	600
75 - 117	SAND (2)	120	850
117 - 140	SAND (2)	120	1000
140 - 180	SAND (2)	130	1200
180 - 250	SAND (2)	130	1500
250	BASE	135	2500

* Water Table at 10 Feet.

TABLE 10. SOIL PROPERTIES AT TACOMA SITE: 3rd PROFILE

Depth, ft.	Soil Type (Mat. Curve)	Unit Weight pcf	Low Strain Shear Wave Velocity (at 10^{-4}%), fps
0 - 10 *	FILL (2)	120	400
10 - 18	SAND (2)	120	400
18 - 35	CLAY (1)	120	400
35 - 60	SAND (2)	120	470
60 - 75	SAND (2)	120	1260
75 - 117	SAND (2)	120	850
117 - 140	SAND (2)	120	1000
140 - 180	SAND (2)	130	1200
180 - 250	SAND (2)	130	1500
250	BASE	135	2500

* Water Table at 10 Feet.

TABLE 11. PROPERTIES OF OCTAGONAL PC PILES

Pile Size in.	Cross-sectional Area, in^2	Moment of Inertia in^4	Concentrated Mass* (at the top), ton
14	162	2105	60
18	268	5750	110
24	477	18,180	200

Unit Weight = 150 pcf

Modulus of Elasticity = 4750 psi

Poisson's Ratio = 0.15

* Unless noted otherwise

TABLE 12. SOIL PROPERTIES AT SAN FRANCISCO SITE

Depth, ft.	Soil Type (Mat. Curve)	Unit Weight pcf	Low Strain Shear Wave Velocity (at 10^{-4}%), fps
0	Sand (2) ▽	125	500
	Sand (2) ⏥	125	800
50	Clay (1)	110	580
100	Clay (1)	125	810
	Clay (1)	130	1120
	Sand (2)	115	1030
150	Clay (1)	130	1170
200			
250	Sand & Gravel (2)	130	1860
285			

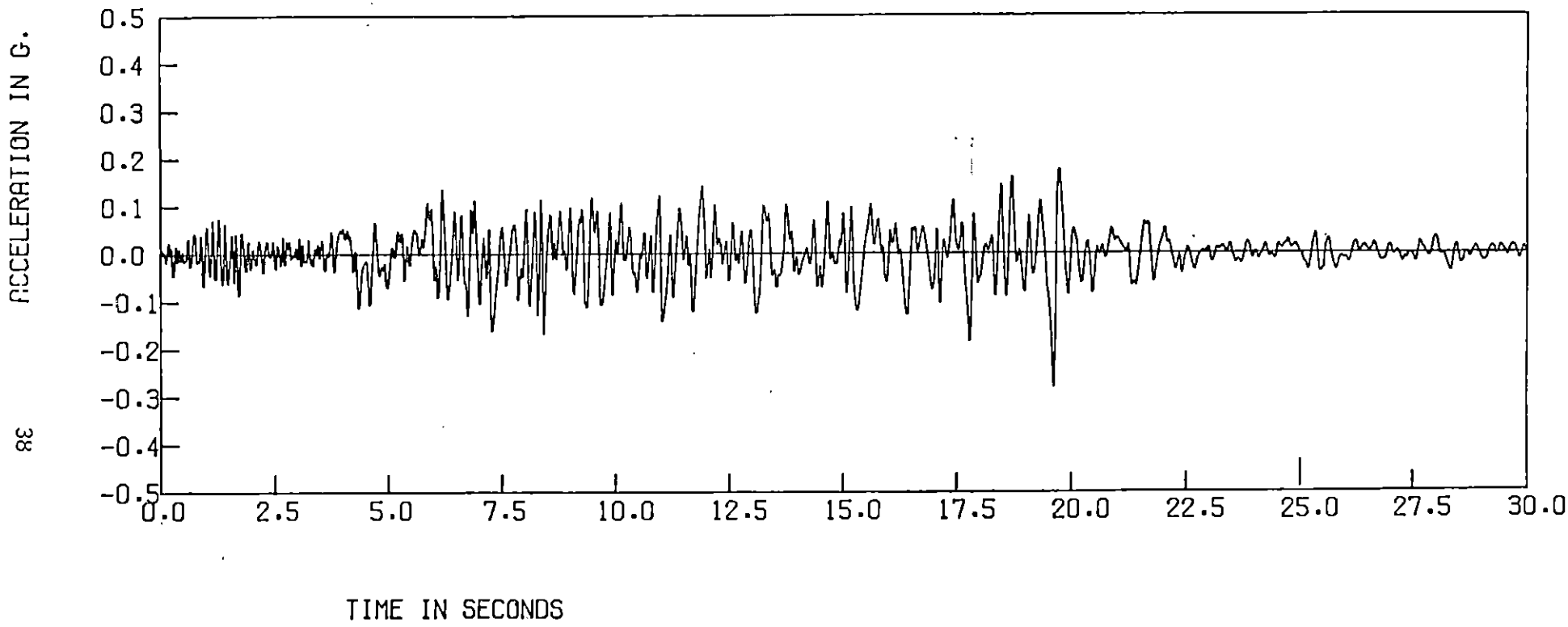

FIGURE 1: EARTHQUAKE RECORD AT OLYMPIA 4/13/49 N86E

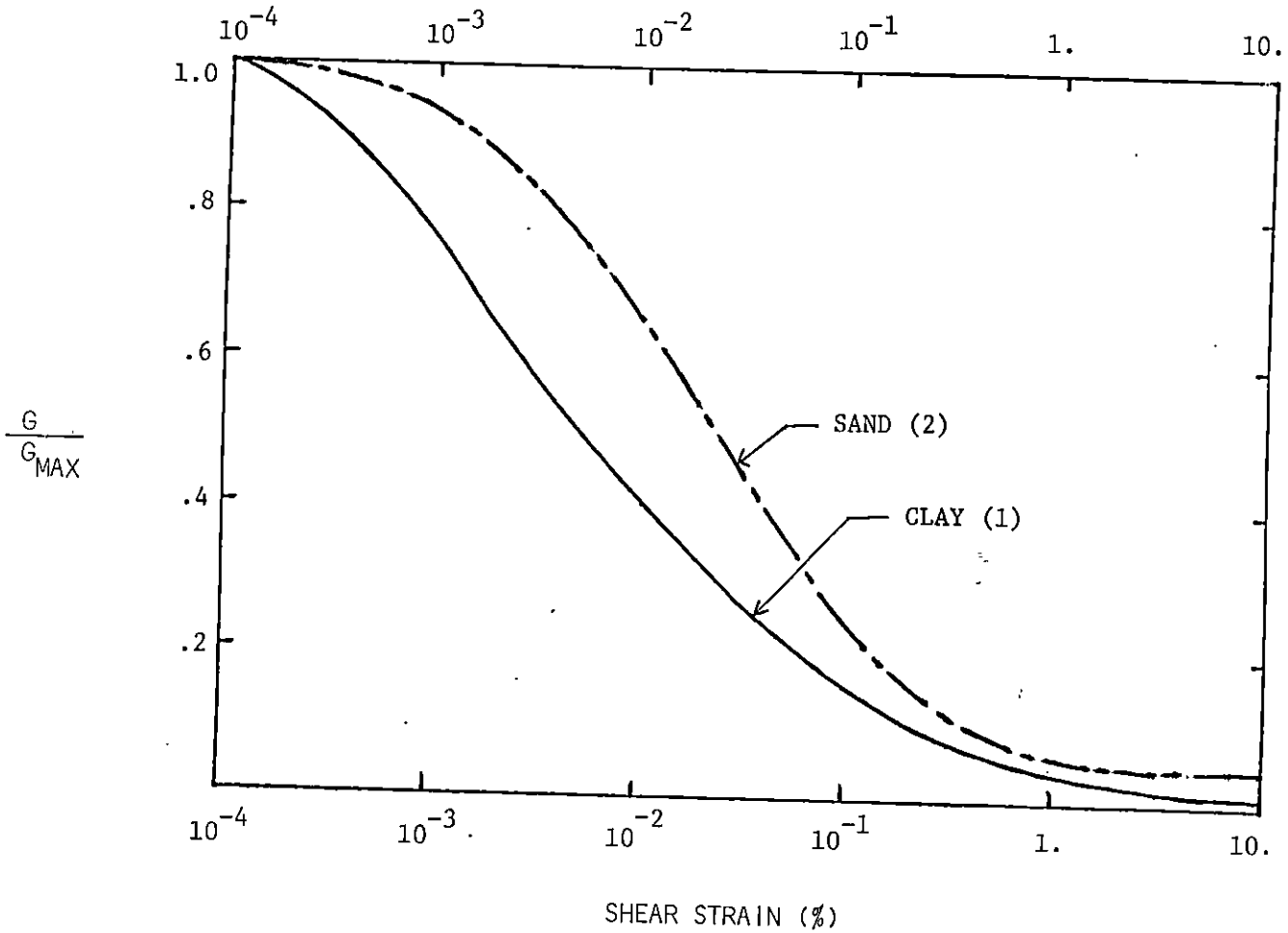

FIGURE 2: EMPIRICAL MODULUS REDUCTION CURVES FOR SOILS

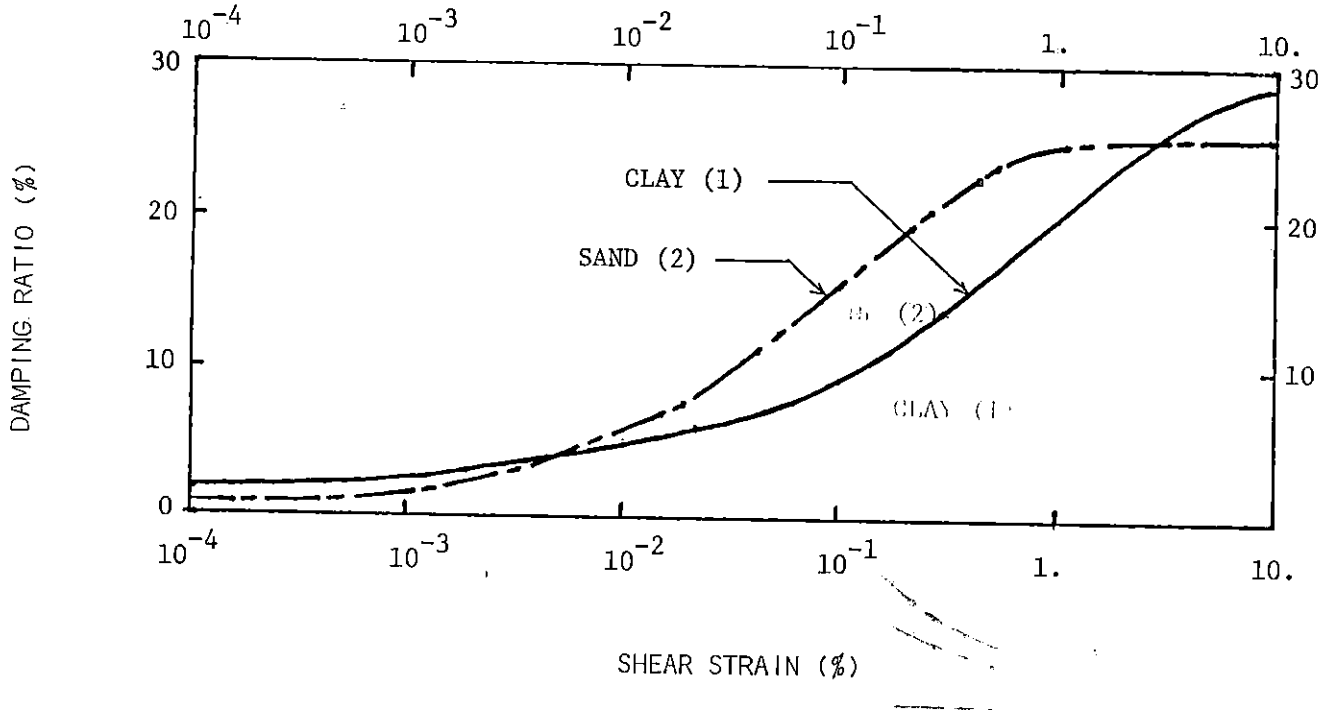

FIGURE 3: EMPIRICAL DAMPING VALUES FOR SOILS

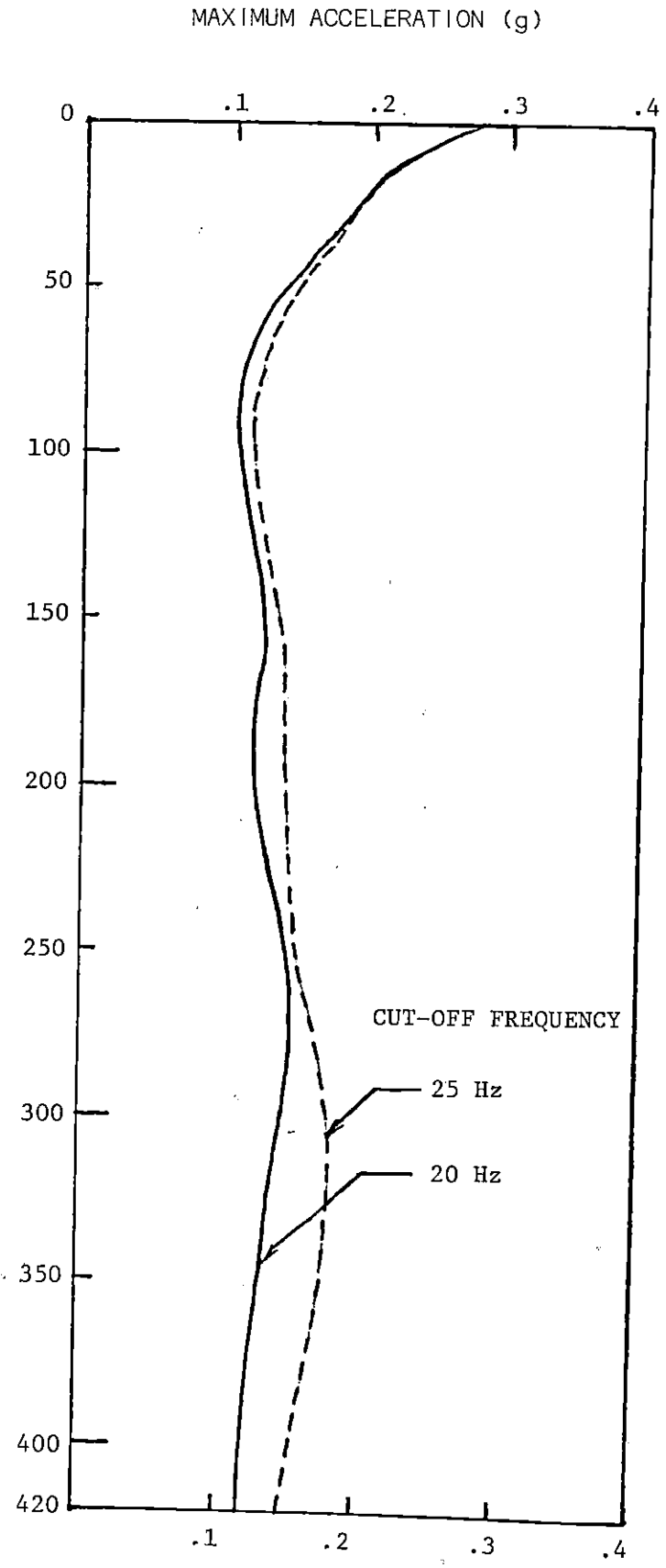

FIGURE 4: PEAK ACCELERATION VS. DEPTH
(DECONVOLUTION ANALYSIS: OLYMPIA HIGHWAY TEST LAB)

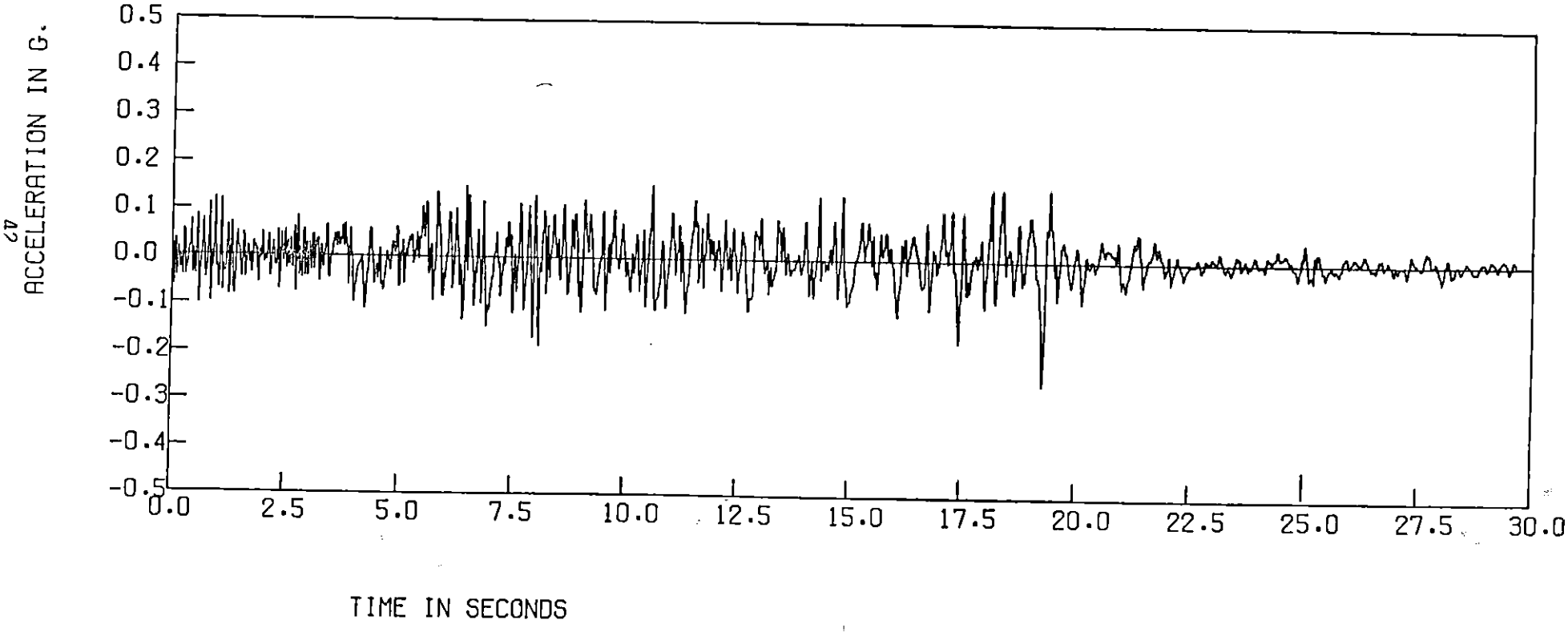

FIGURE 5: CONTROL MOTION AT 250 FT. (OUTCROPPING)

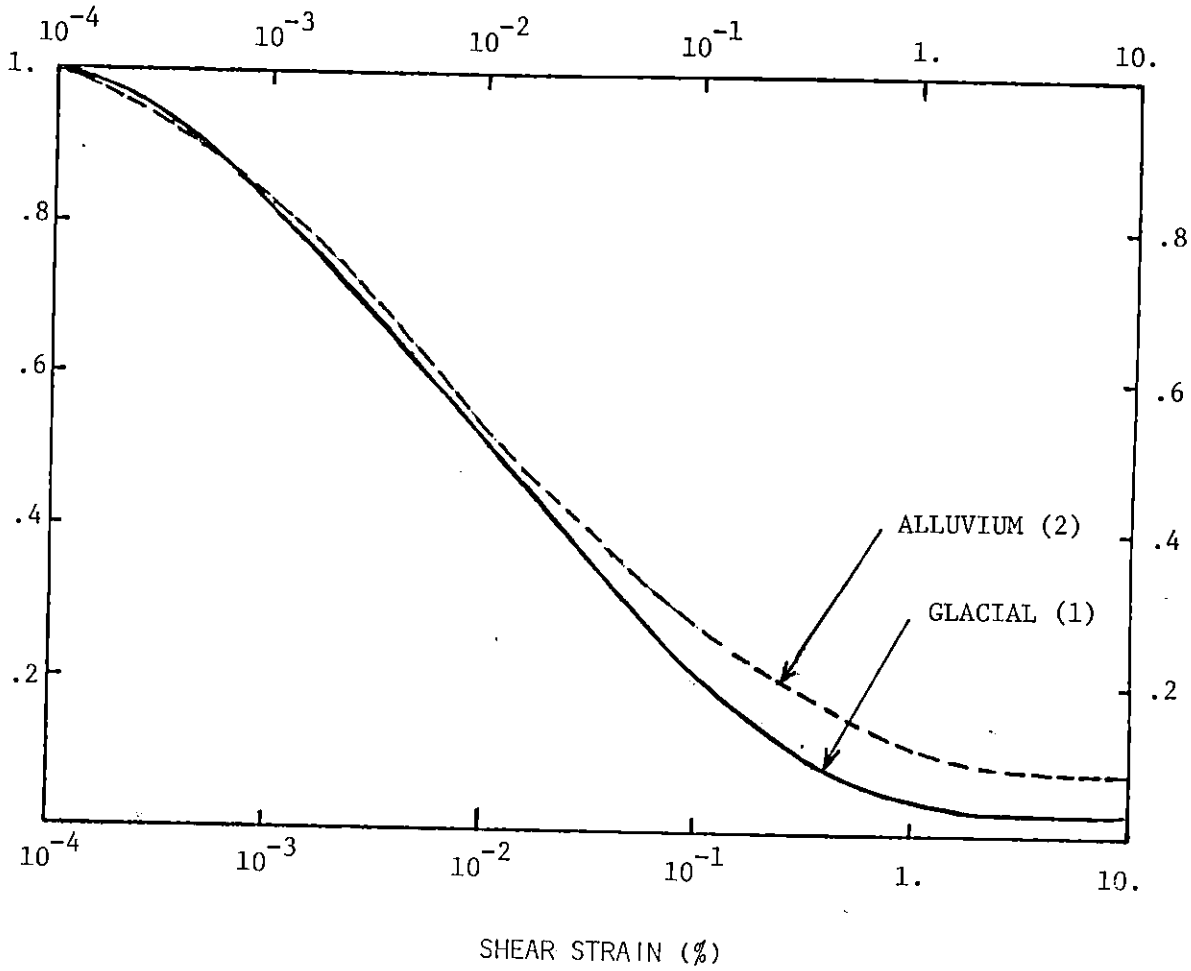

FIGURE 6: MODULUS REDUCTION CURVES FOR WEST SEATTLE SOILS

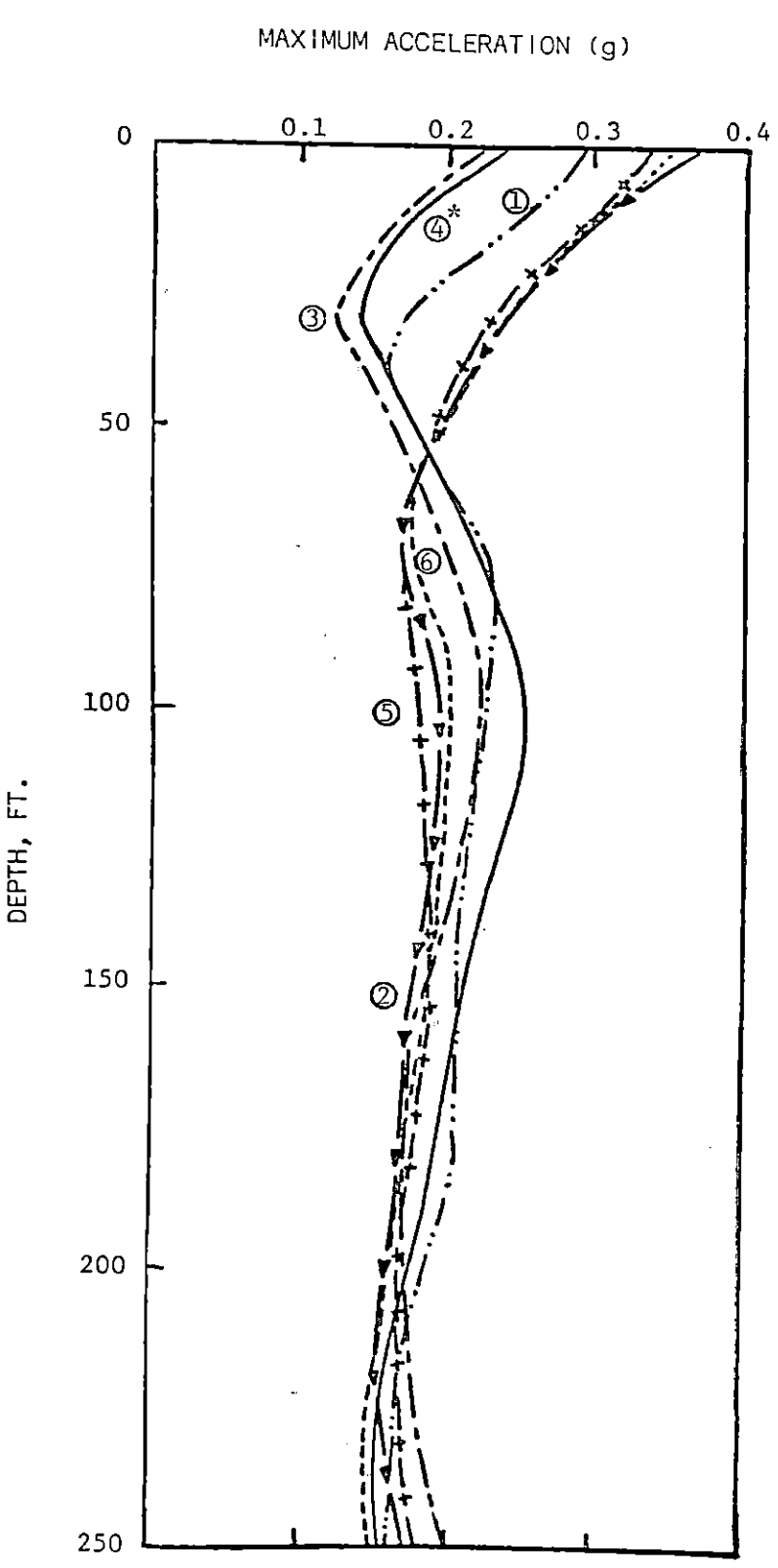

* Circled numbers within the graph denote the profile used for analysis

FIGURE 7: PEAK ACCELERATION VS. DEPTH (FREE-FIELD ANALYSIS: WEST SEATTLE SITE)

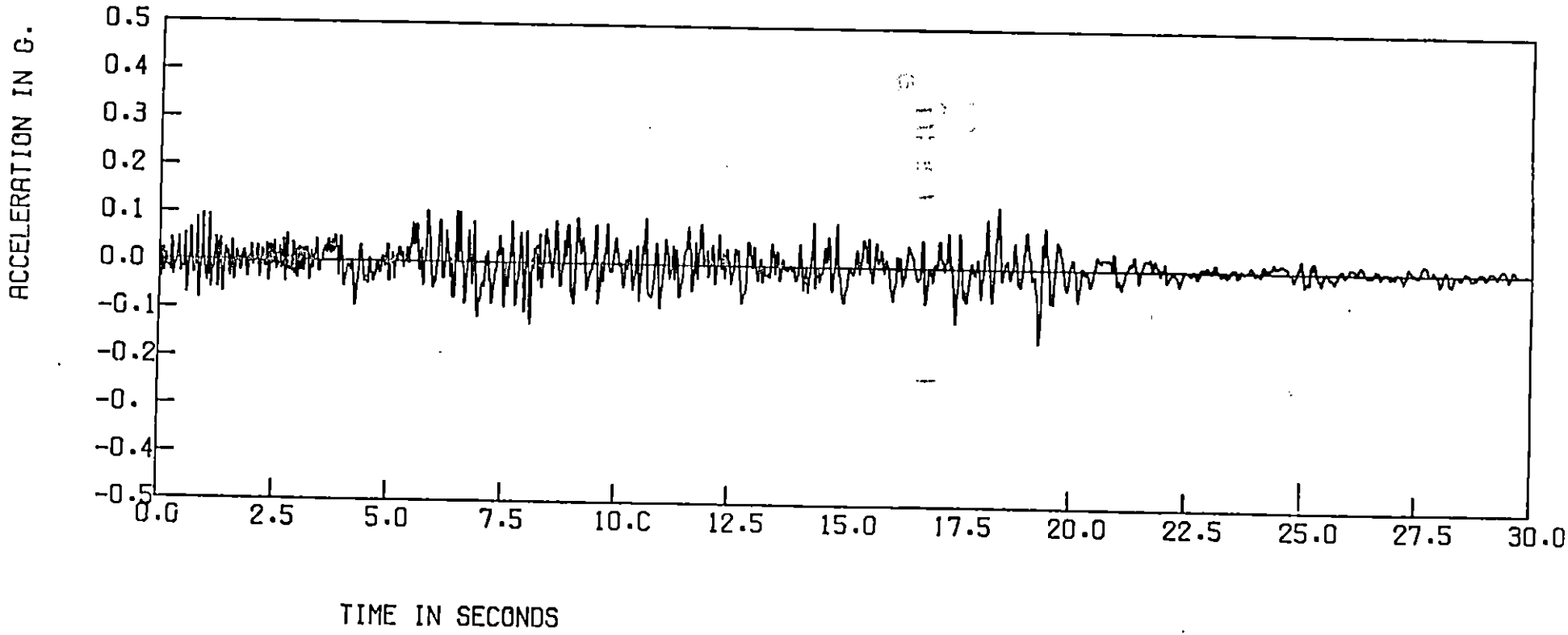

FIGURE 8: BASE MOTION AT 250 FT. (4TH PROFILE, WEST SEATTLE)

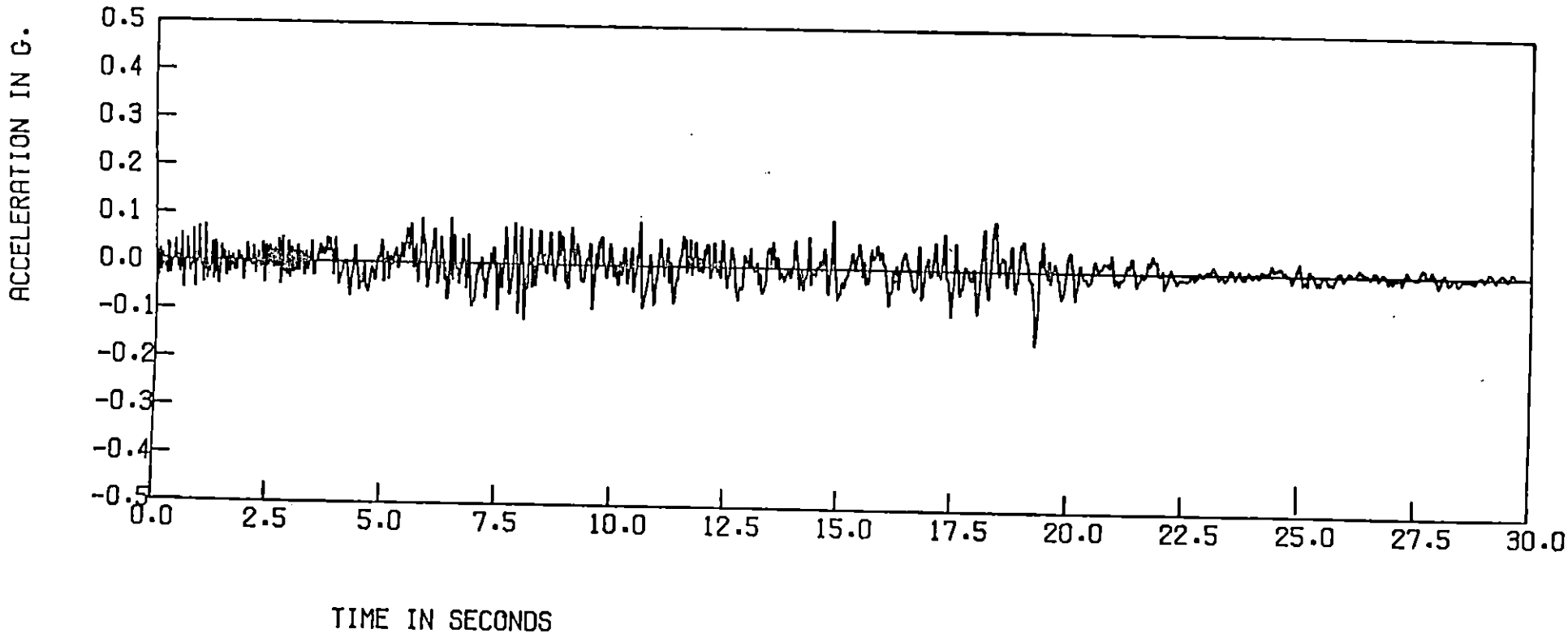

FIGURE 9: BASE MOTION AT 250 FT. (6TH PROFILE, WEST SEATTLE)

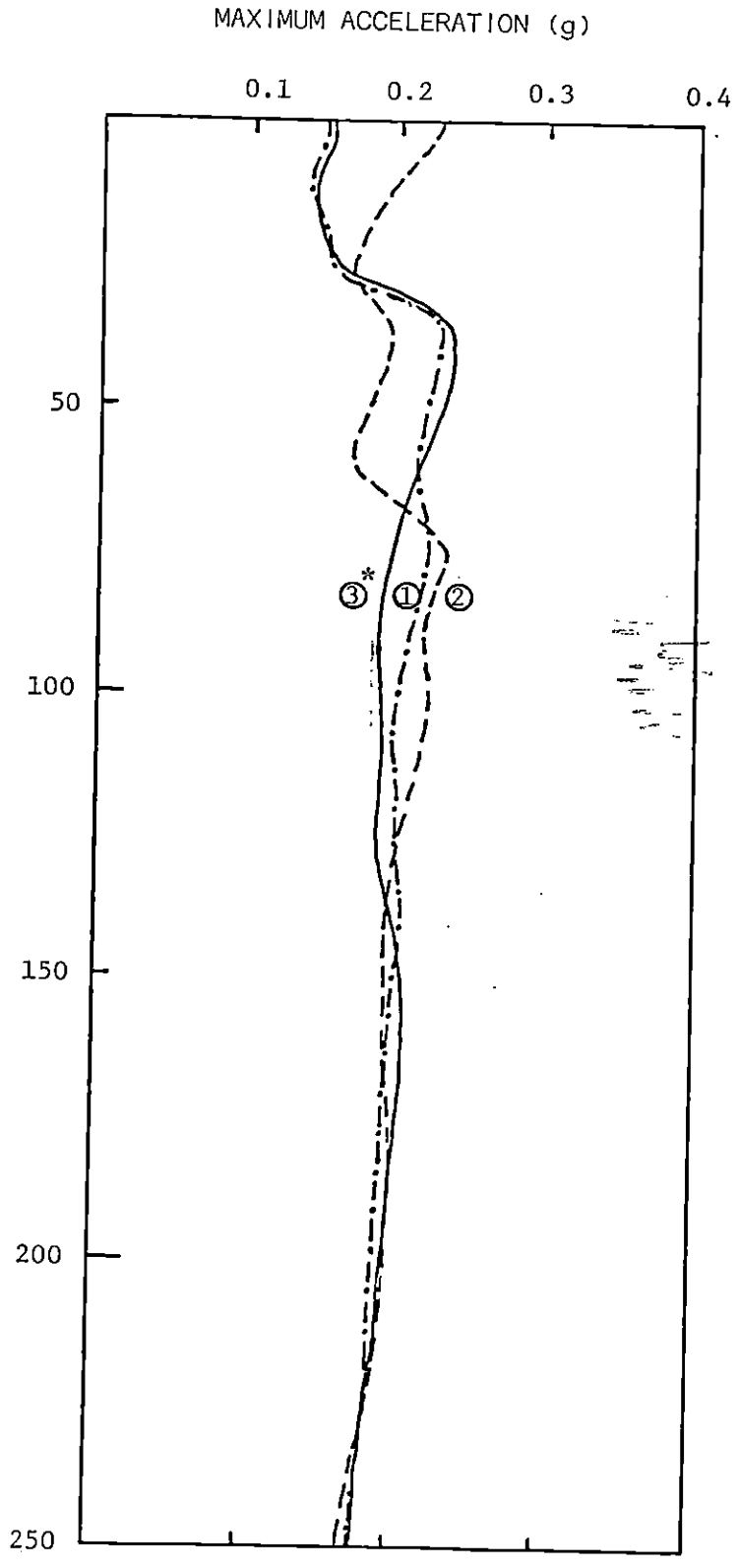

* Circled numbers within the graph denote the profile used for analysis

FIGURE 10: PEAK ACCELERATION VS. DEPTH (FREE-FIELD ANALYSIS: TACOMA SITE)

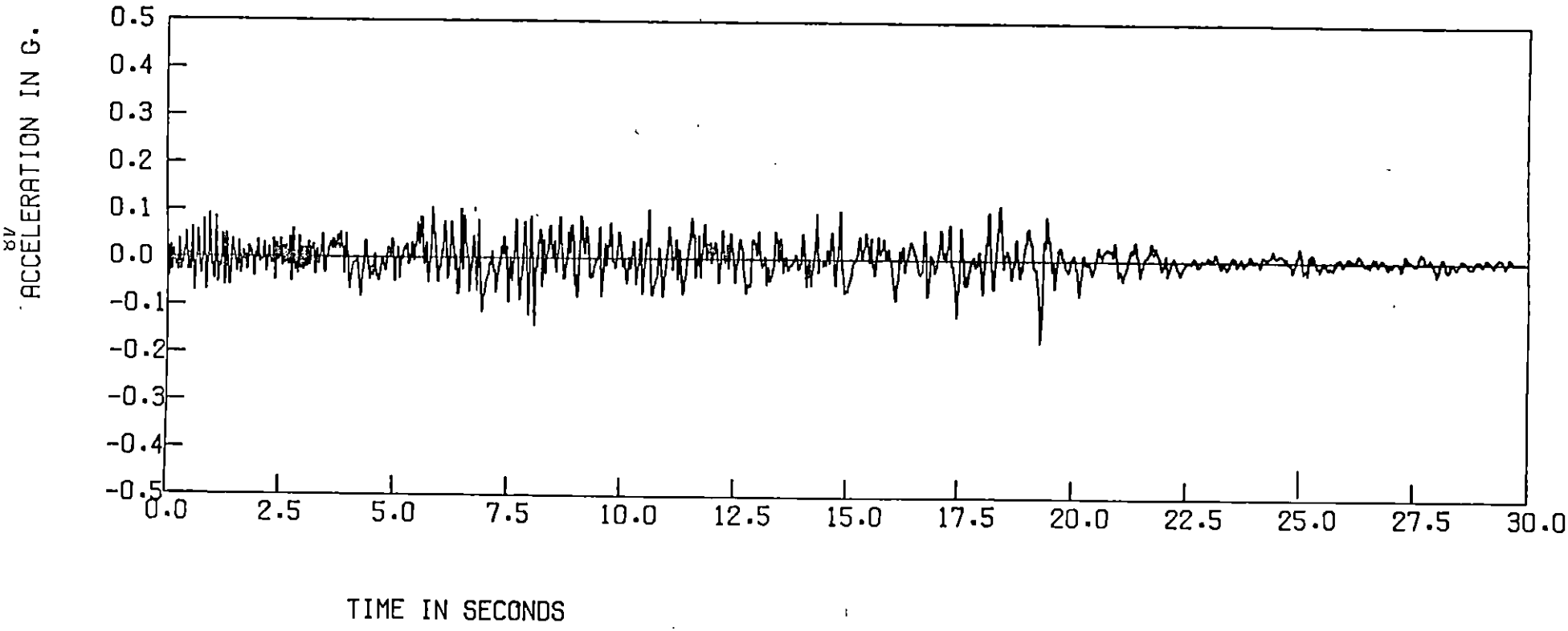

FIGURE 11: BASE MOTION AT 250 FT. (2ND PROFILE, TACOMA)

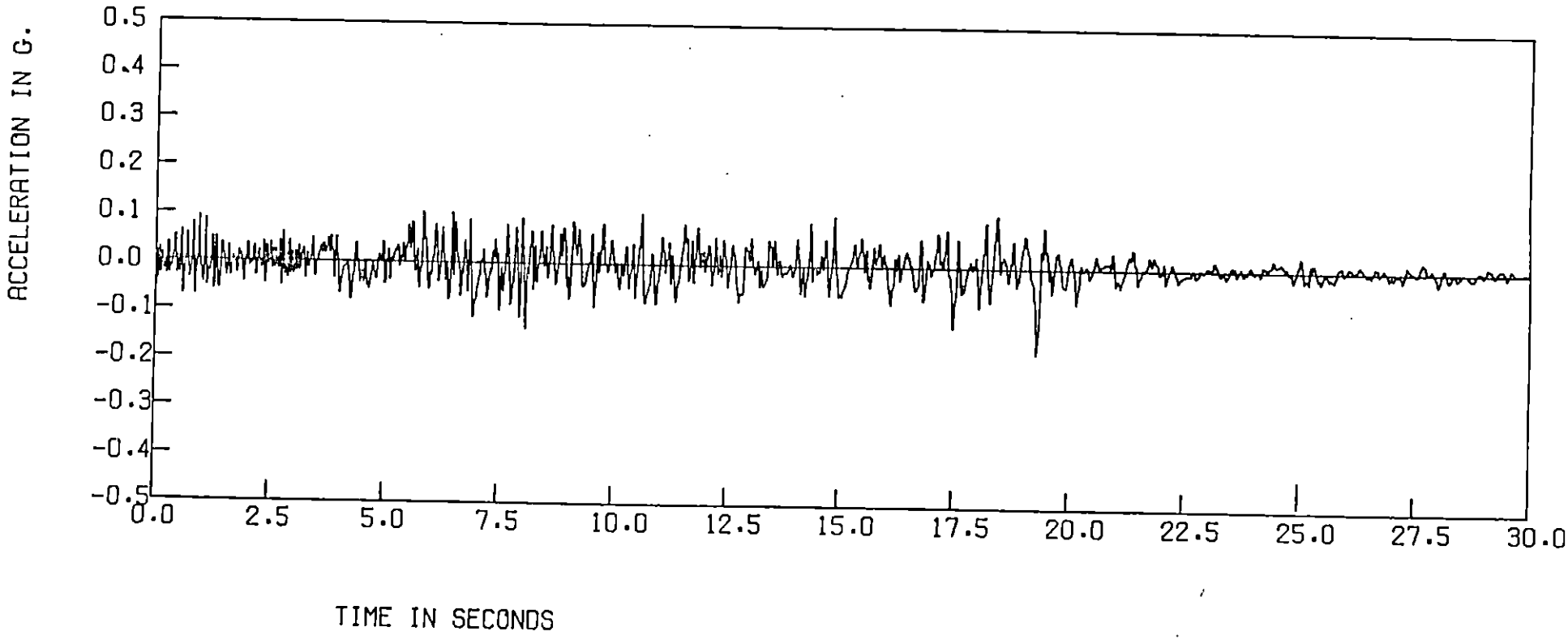

FIGURE 12: BASE MOTION AT 250 FT. (3RD PROFILE, TACOMA)

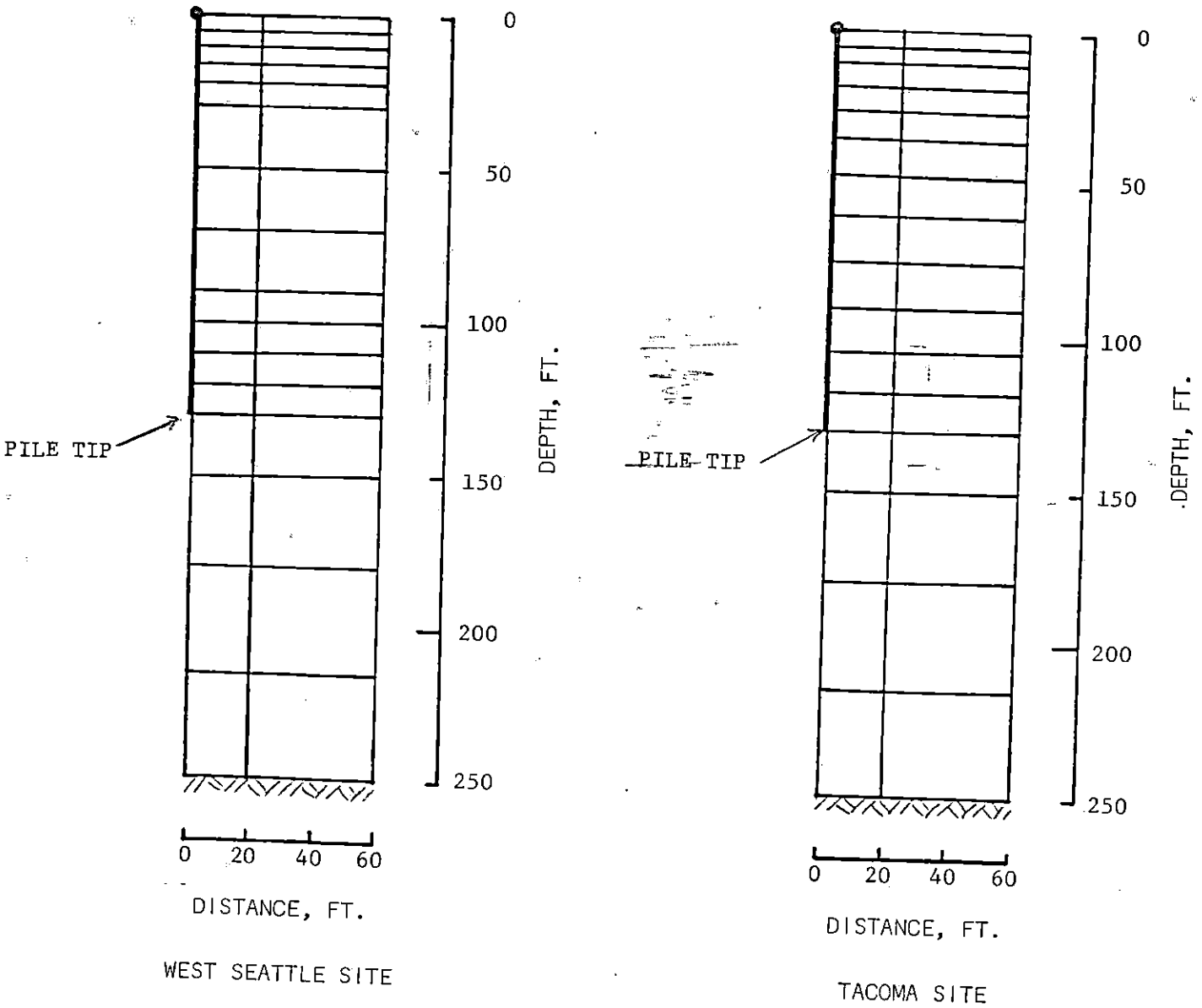

FIGURE 13: FINITE ELEMENT MESHES USED FOR SOIL-PILE INTERACTION ANALYSES

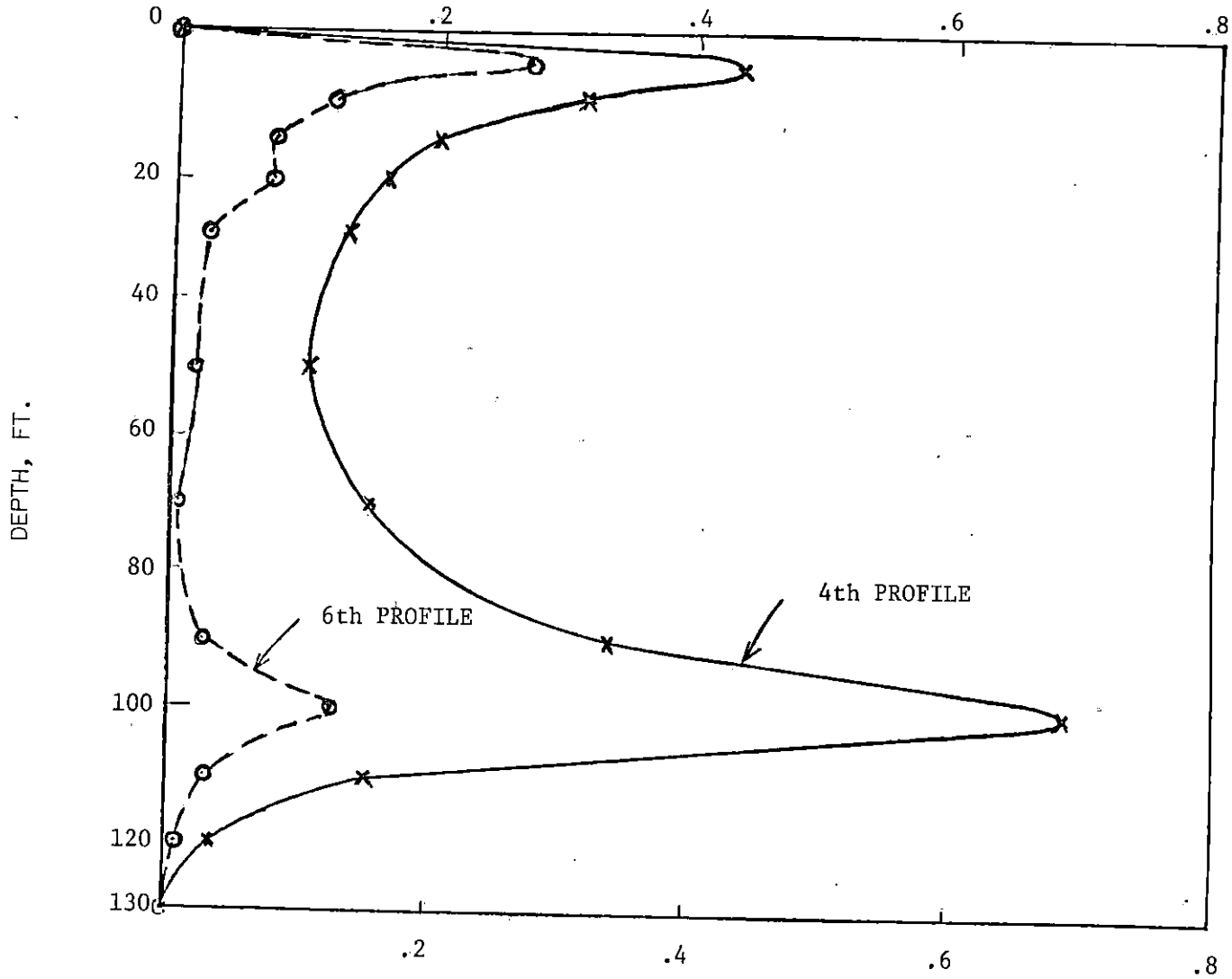

FIGURE 14: MAXIMUM INDUCED CURVATURES ON 14-INCH OCTAGONAL PILE (WEST SEATTLE SITE; FREE END CONDITION)

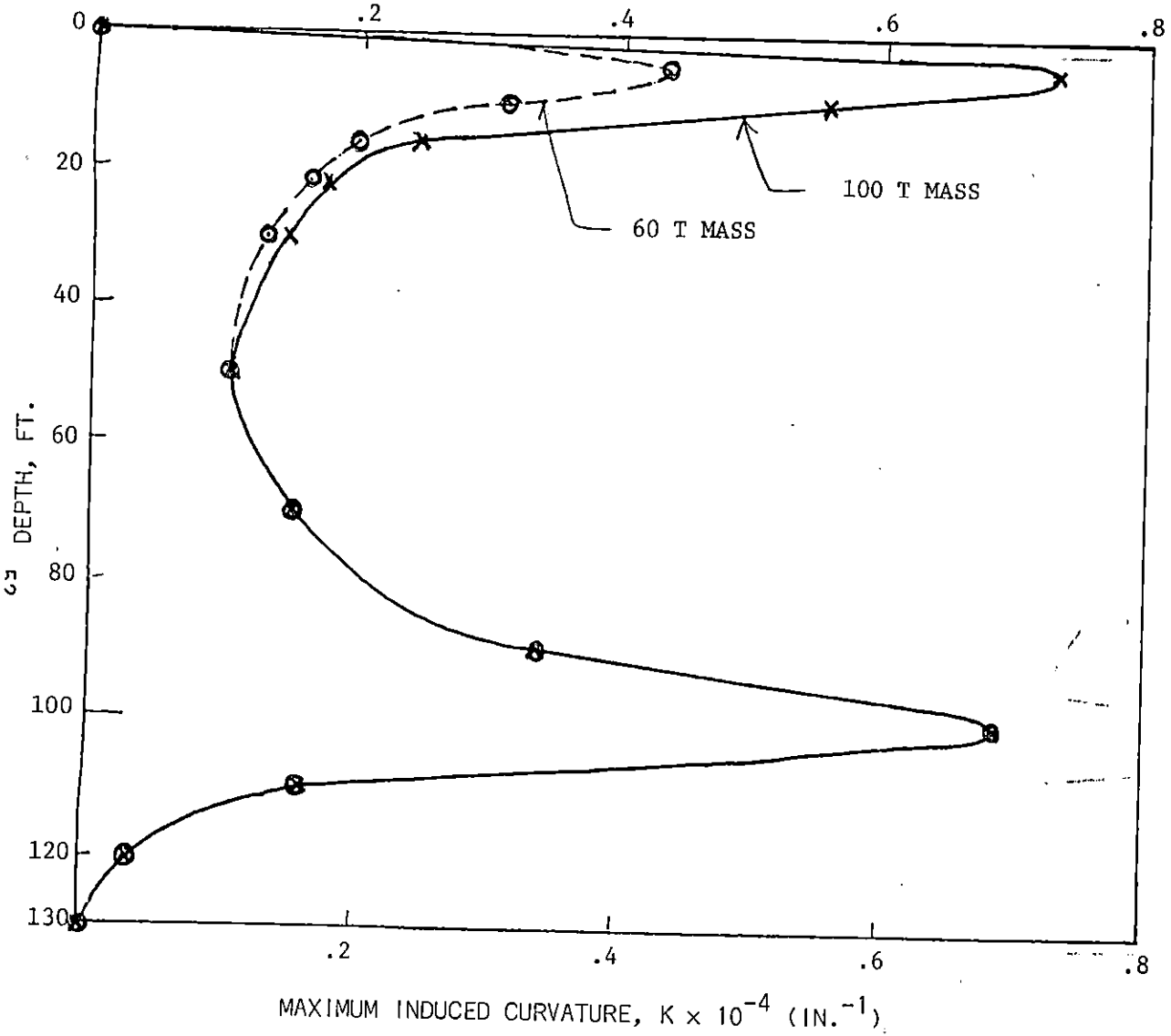

FIGURE 15: EFFECT OF THE SIZE OF PILE CAP ON INDUCED CURVATURES
(WEST SEATTLE SITE; 4TH PROFILE; FREE END CONDITION)

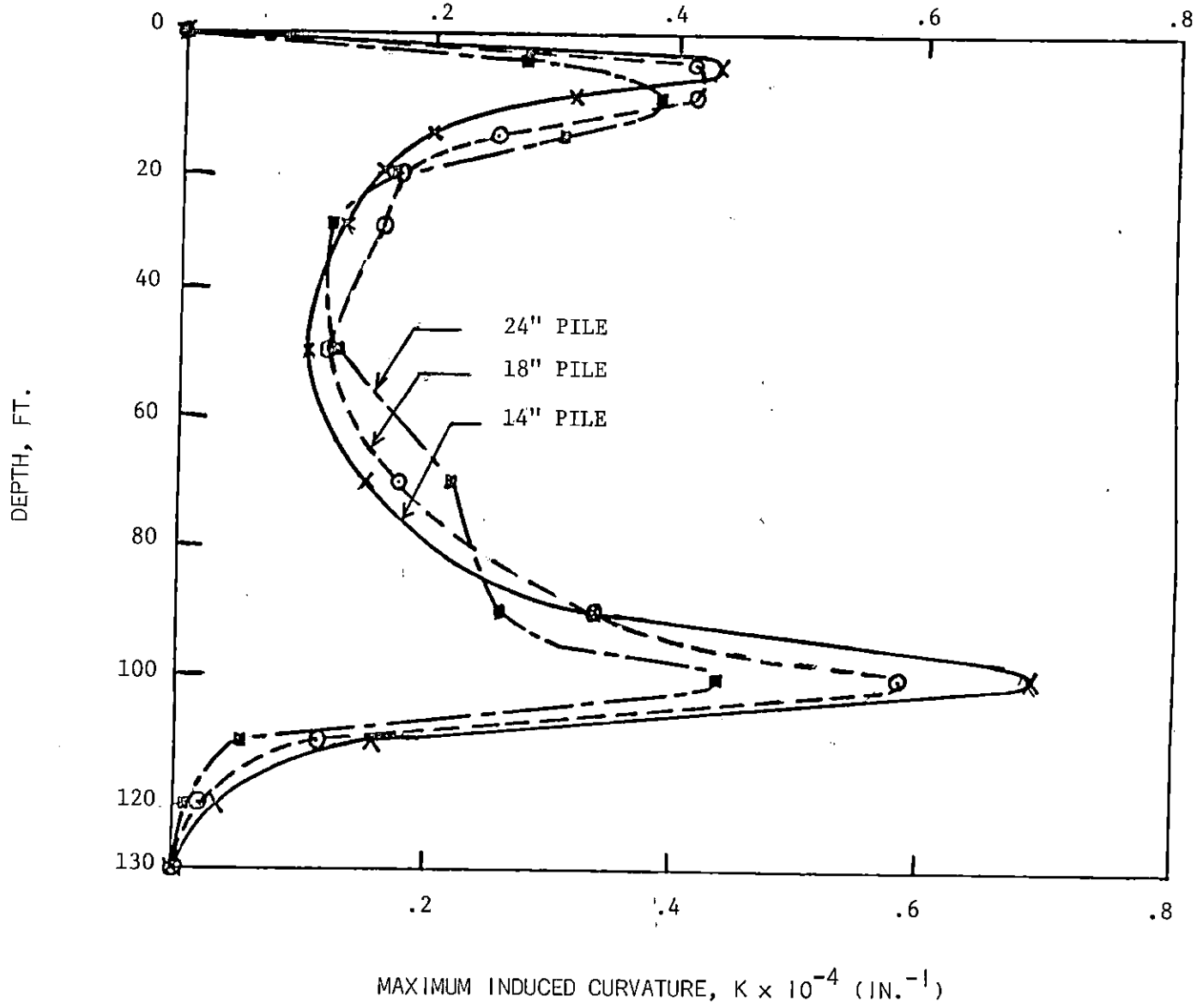

FIGURE 16: EFFECT OF PILE SIZE ON THE INDUCED CURVATURES (WEST SEATTLE SITE; 4TH PROFILE; FREE END CONDITION)

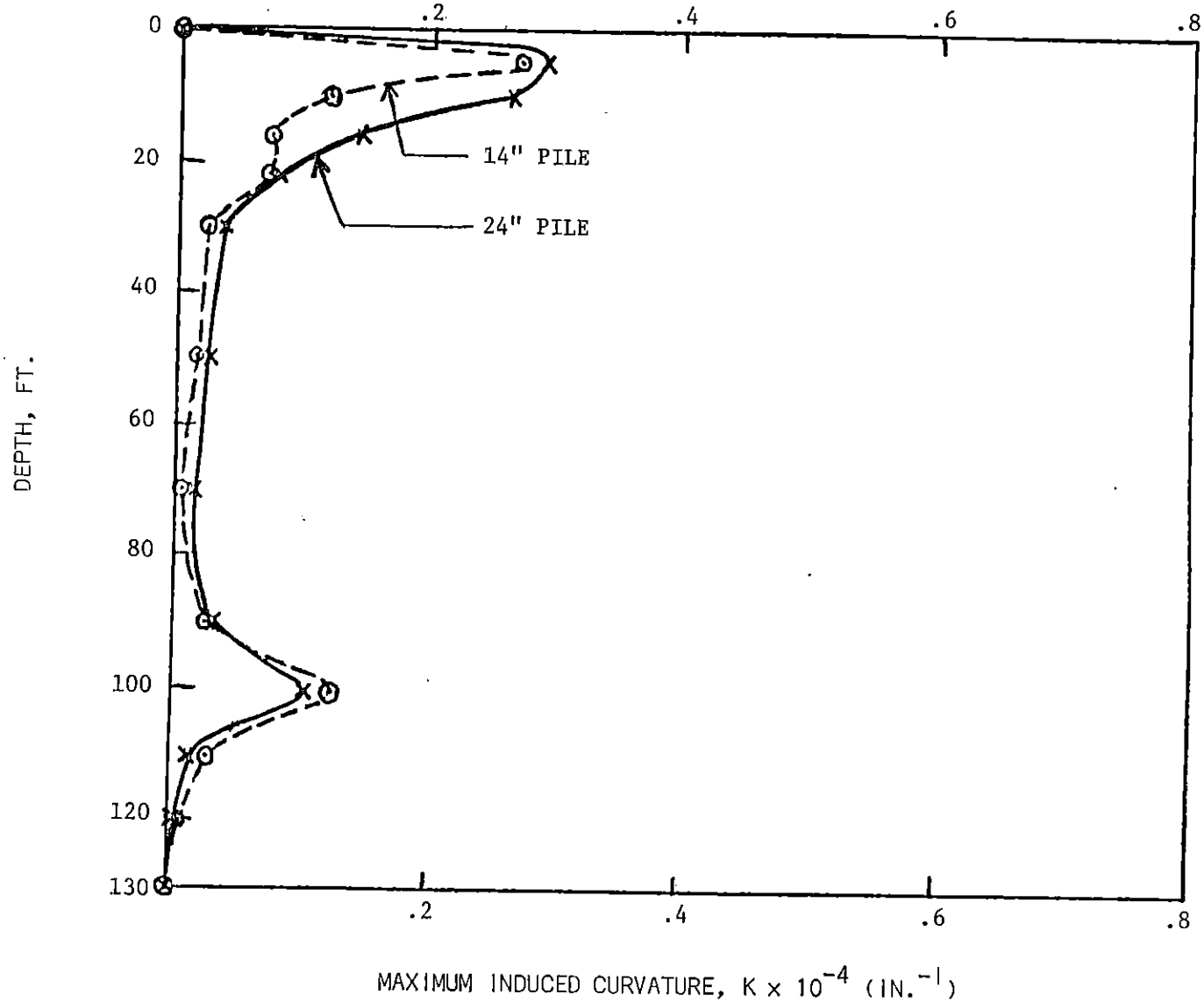

FIGURE 17: EFFECT OF PILE SIZE ON INDUCED CURVATURES (WEST SEATTLE SITE; 6TH PROFILE; FREE END CONDITION)

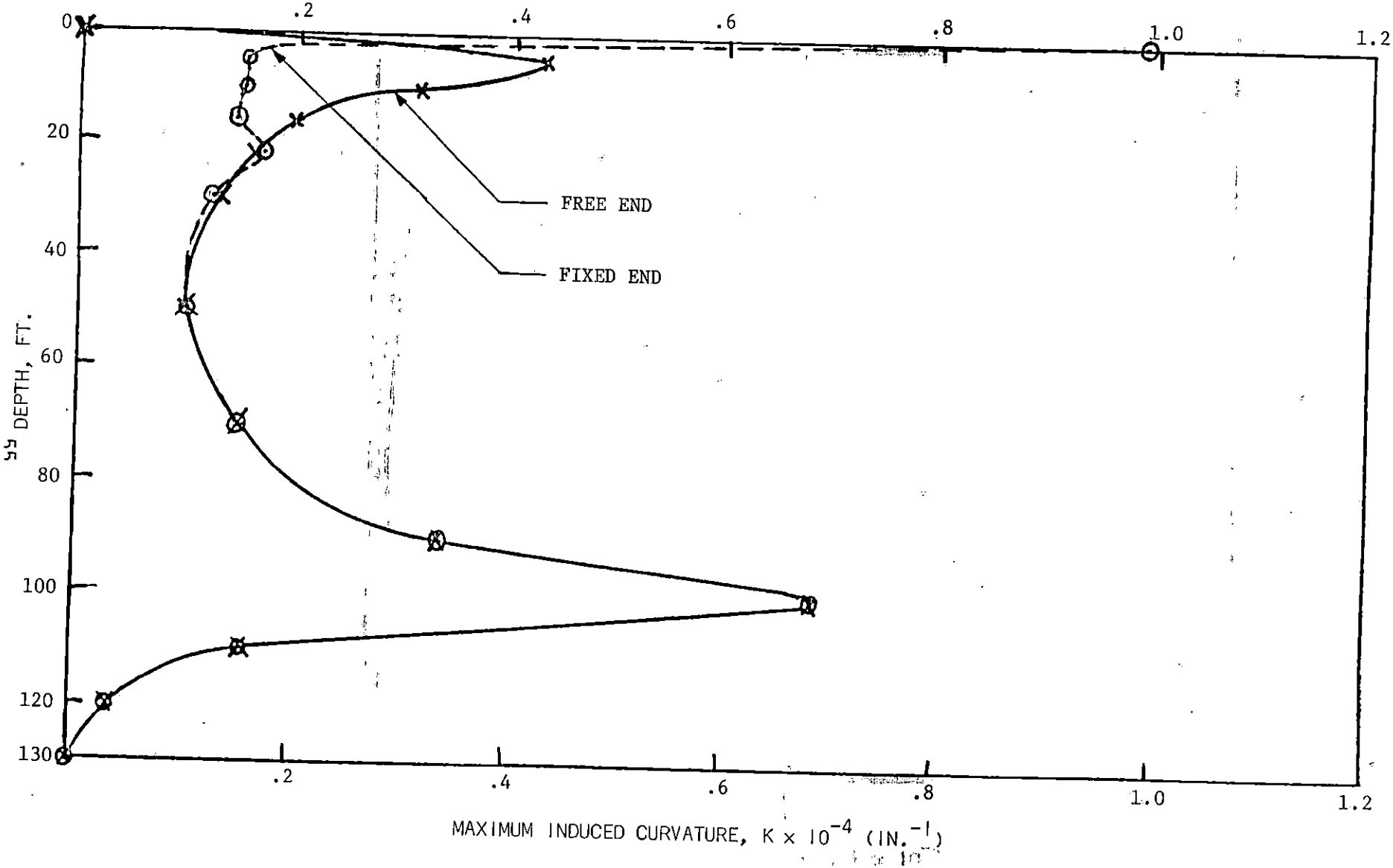

FIGURE 18: EFFECT OF ROTATIONAL FIXITY ON INDUCED CURVATURES (WEST SEATTLE SITE; 4TH PROFILE; 14 IN. PILE SIZE)

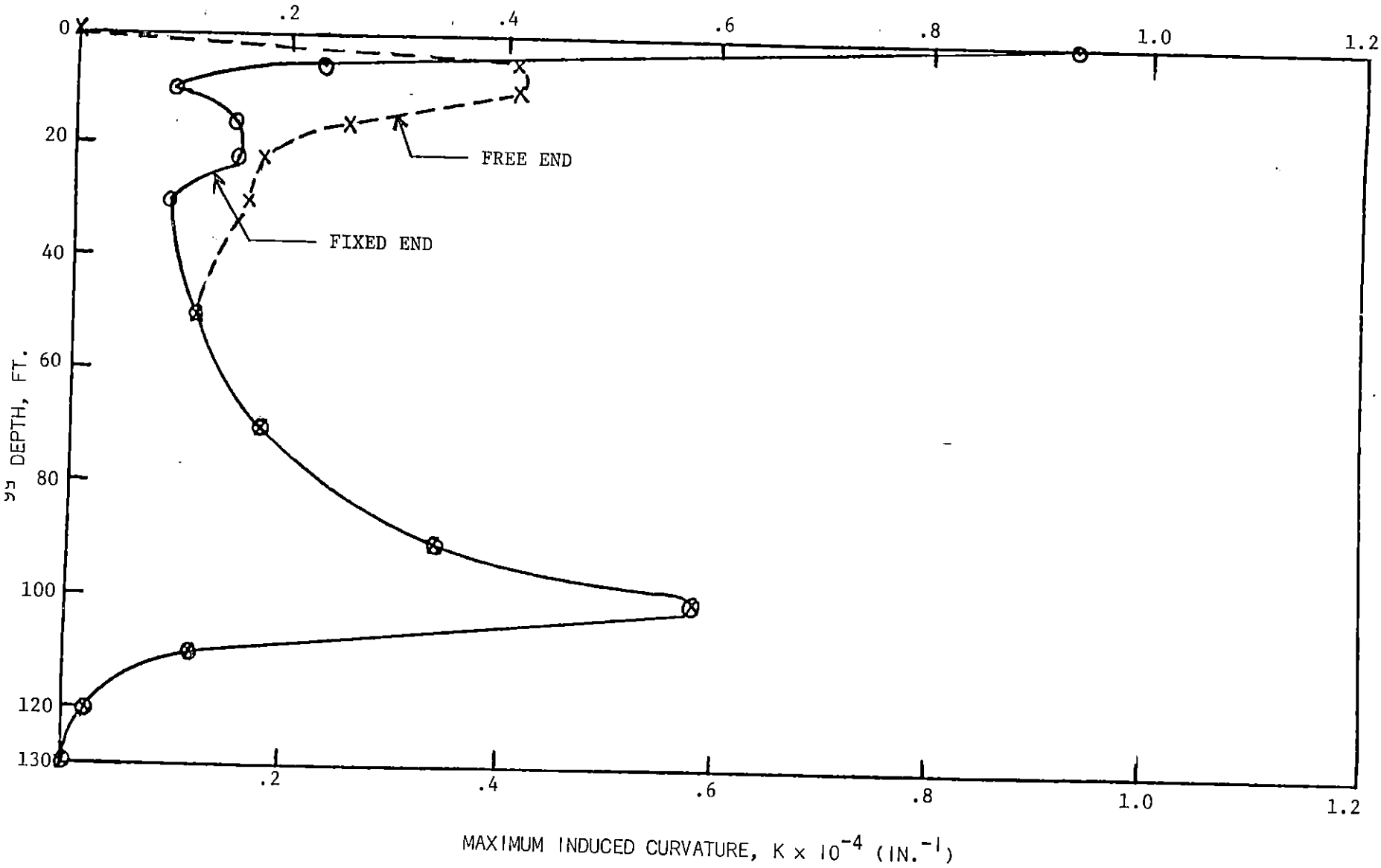

FIGURE 19: EFFECT OF ROTATIONAL FIXITY ON INDUCED CURVATURES (WEST SEATTLE SITE; 4TH PROFILE; 18 IN. PILE SIZE)

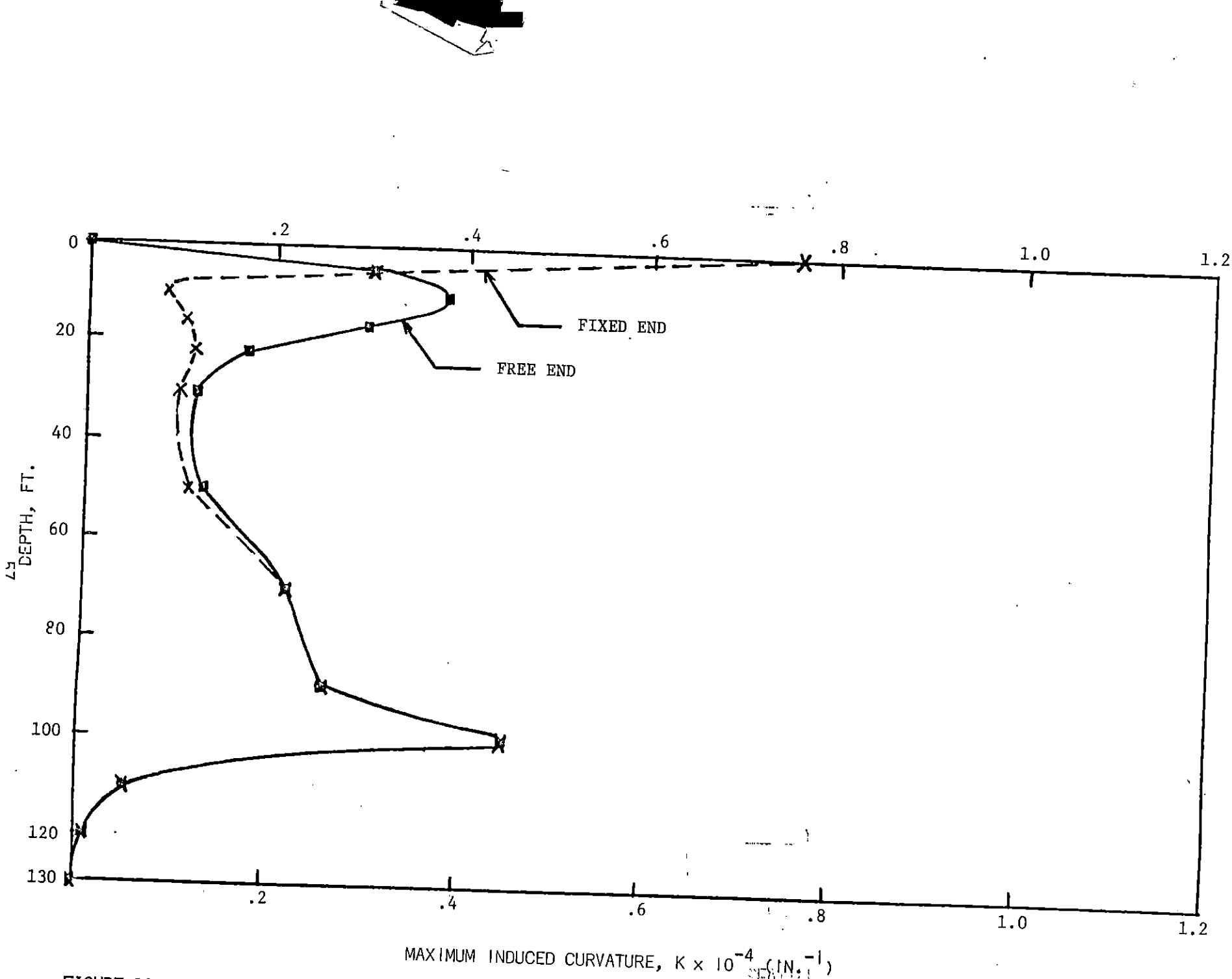

FIGURE 20: EFFECT OF ROTATIONAL FIXITY ON INDUCED CURVATURES (WEST SEATTLE SITE; 4TH PROFILE; 24 IN. PILE SIZE)

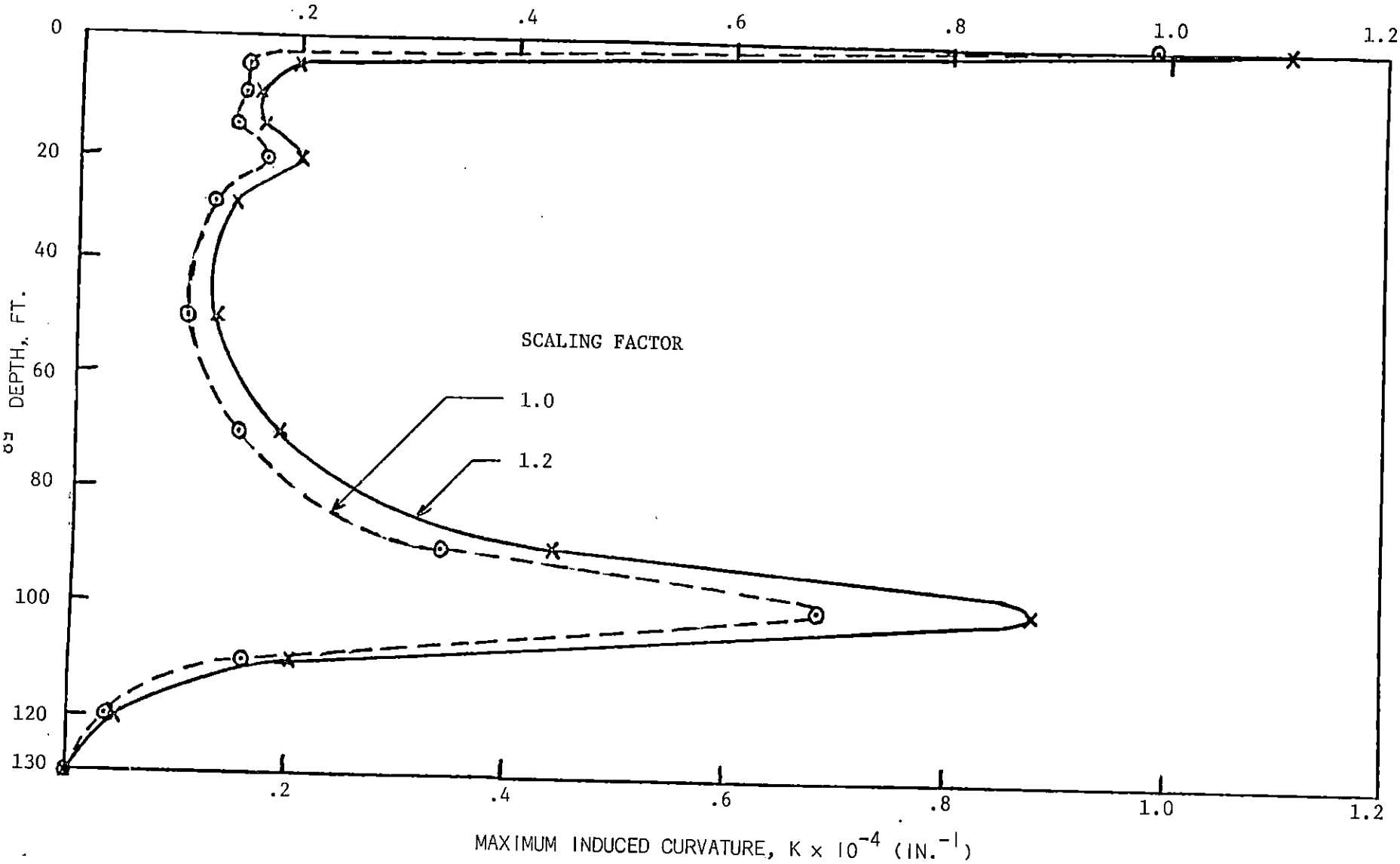

FIGURE 21: EFFECT OF SCALING OF BASE ACCELERATIONS ON INDUCED CURVATURES
(WEST SEATTLE; 4TH PROFILE; 14 IN. PILE SIZE; FIXED END CONDITION)

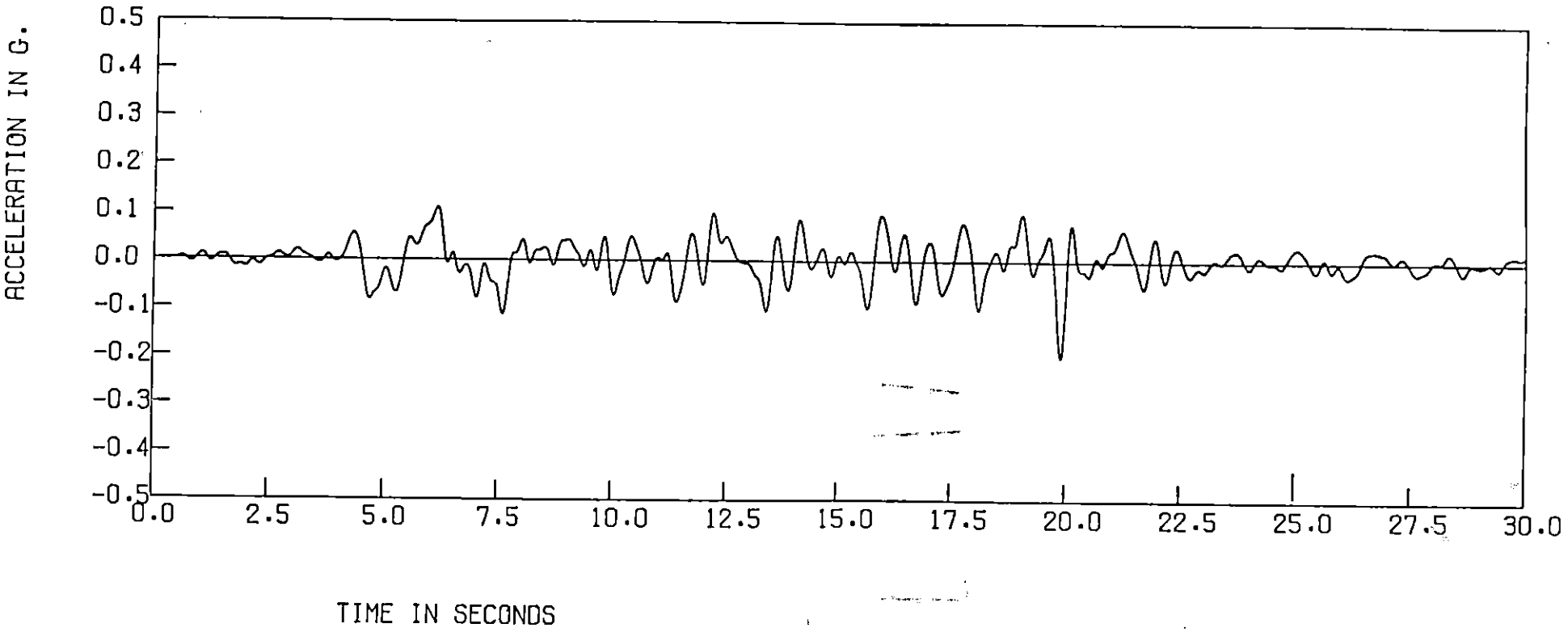

FIGURE 22: MOTION AT TOP OF 14 IN. PILE (4TH PROFILE, WEST SEATTLE)

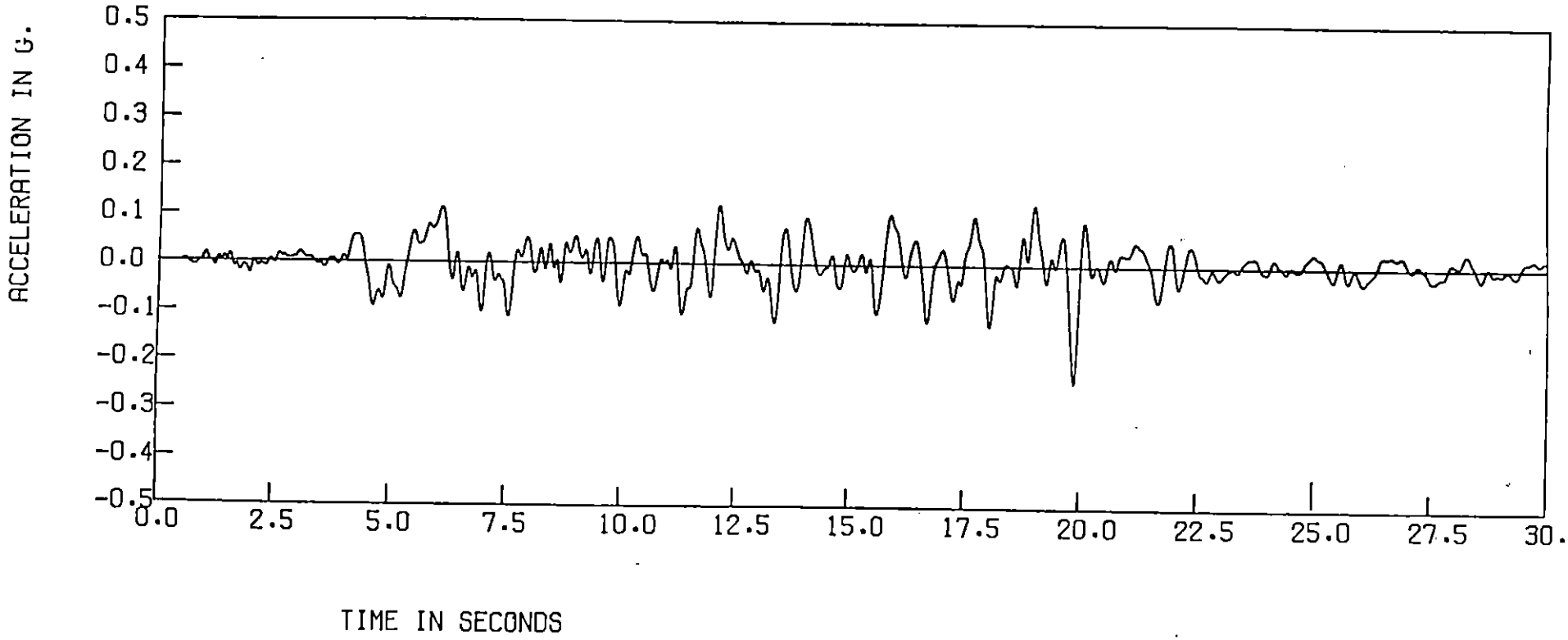

FIGURE 23: GROUND SURFACE MOTION (4TH PROFILE, WEST SEATTLE)

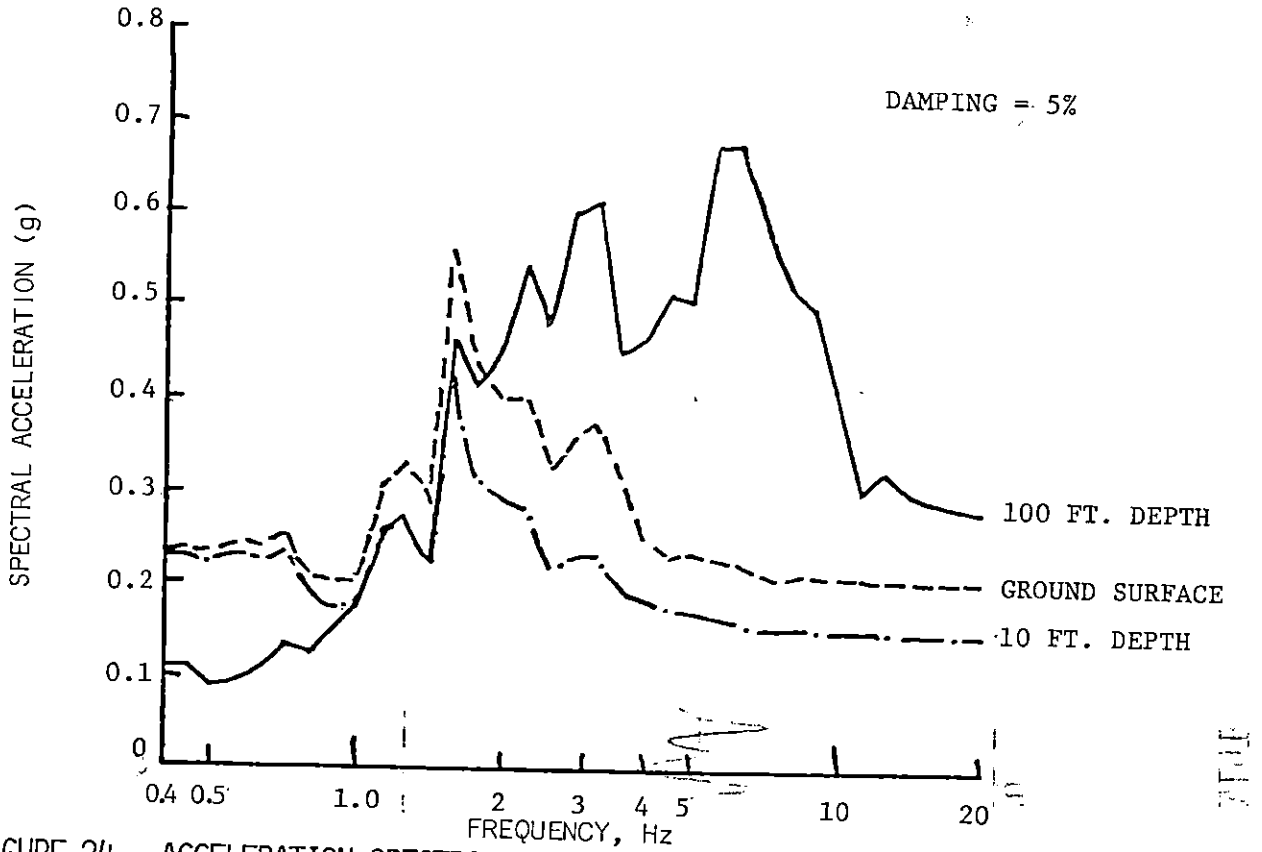

FIGURE 24: ACCELERATION SPECTRA AT VARIOUS DEPTHS ALONG PILE
(WEST SEATTLE SITE; 4TH PROFILE; 14 IN. PILE SIZE)

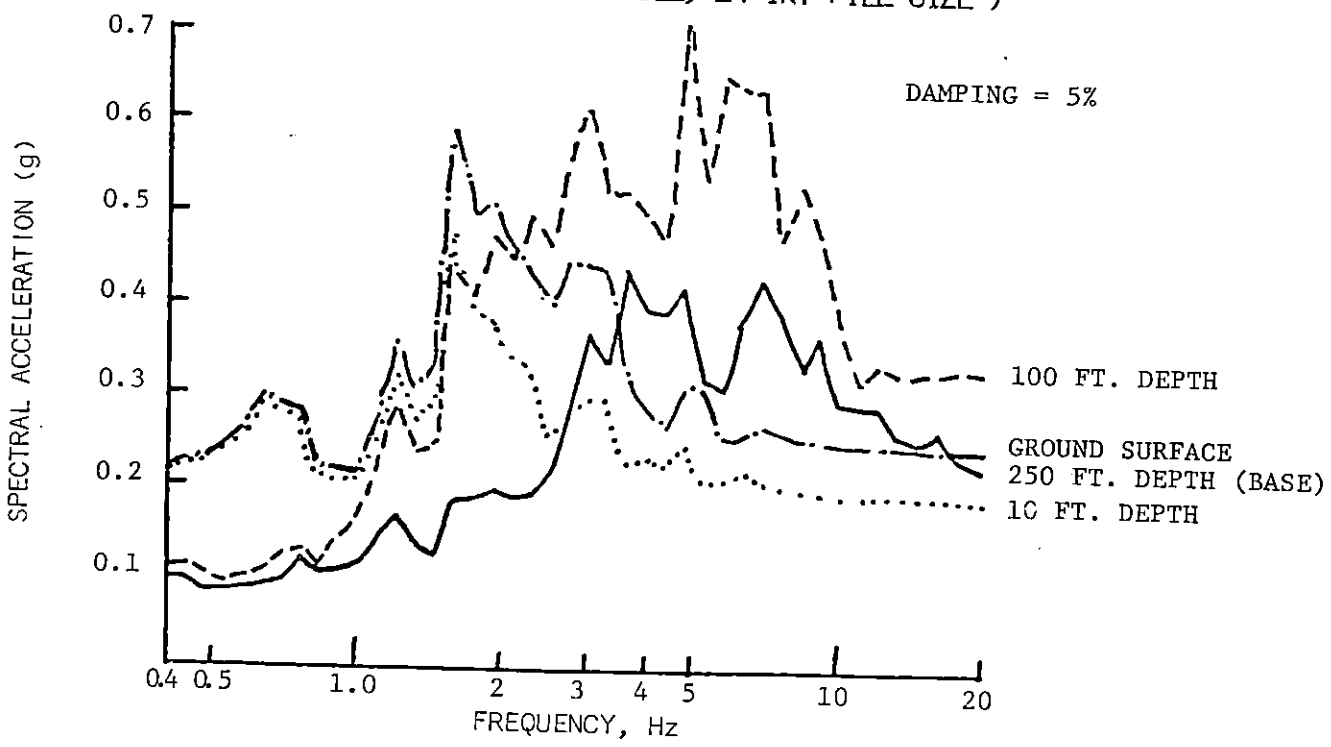

FIGURE 25: ACCELERATION SPECTRA AT VARIOUS DEPTHS IN THE FREE-FIELD
(WEST SEATTLE SITE; 4TH PROFILE)

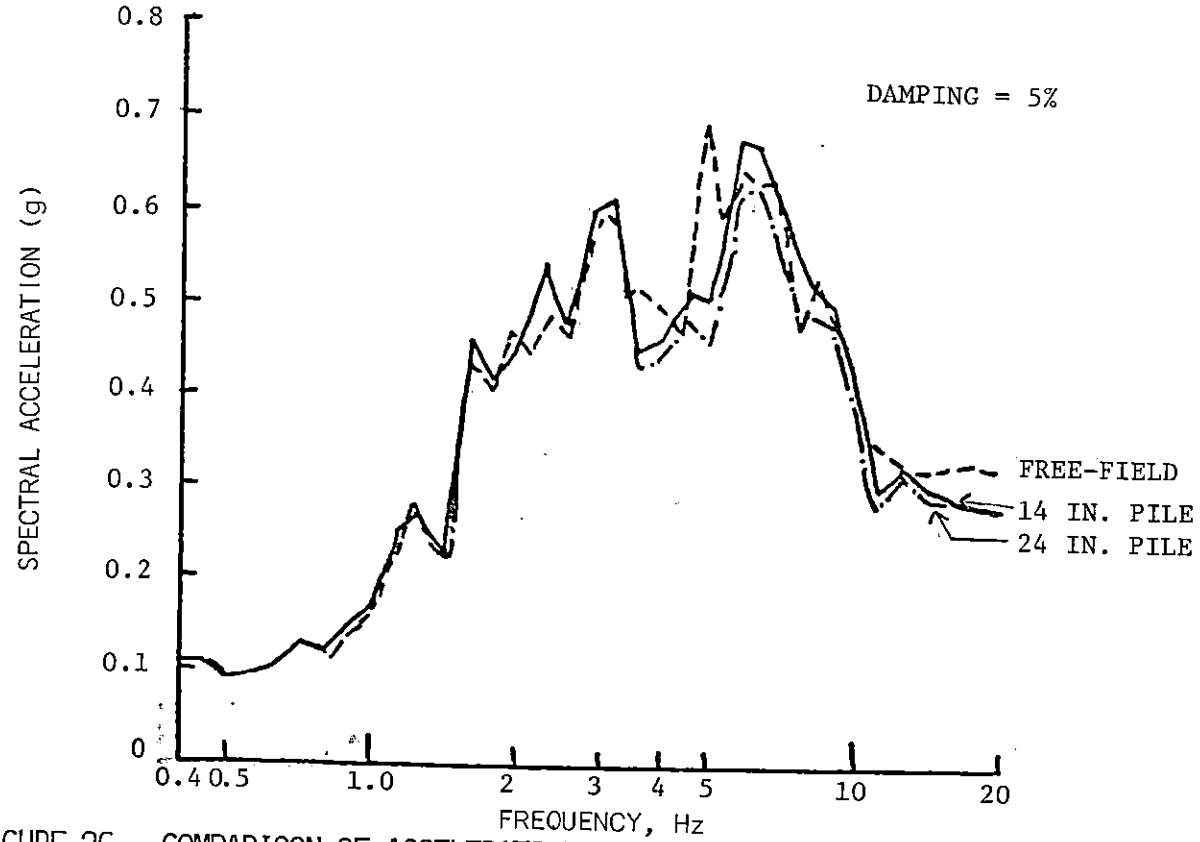

FIGURE 26: COMPARISON OF ACCELERATION SPECTRA AT 100 FT. DEPTH ON THE PILES AND IN THE FREE-FIELD (WEST SEATTLE SITE ; 4TH PROFILE)

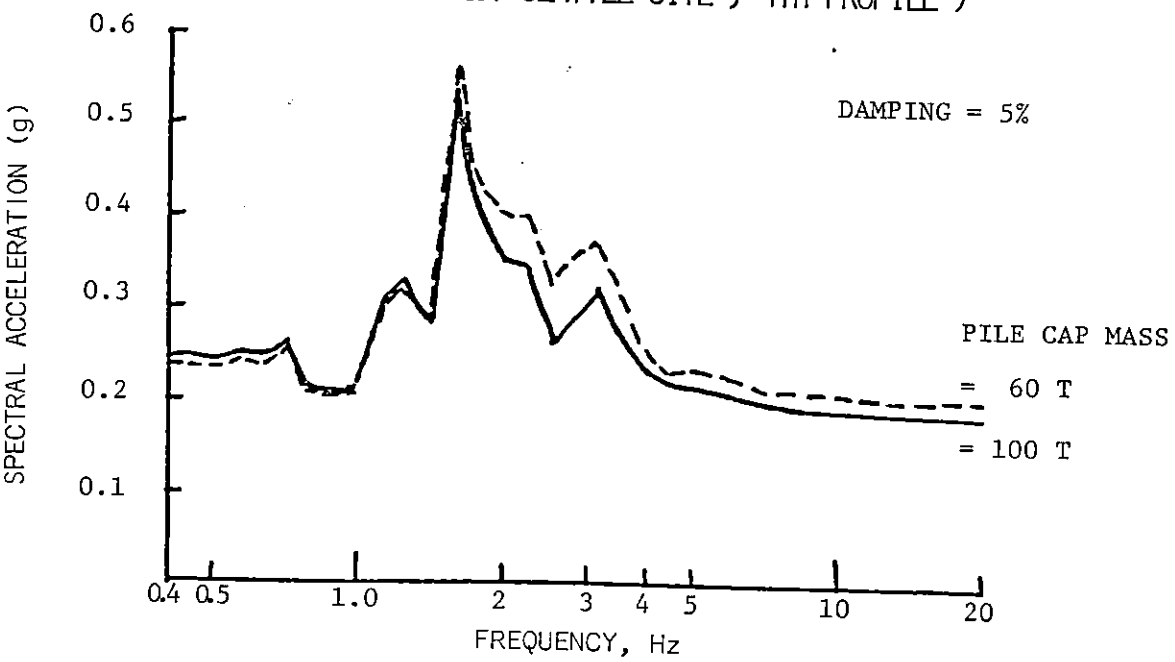

FIGURE 27: ACCELERATION SPECTRA AT THE TOP OF PILE
(WEST SEATTLE SITE; 4TH PROFILE; 14 IN. PILE)

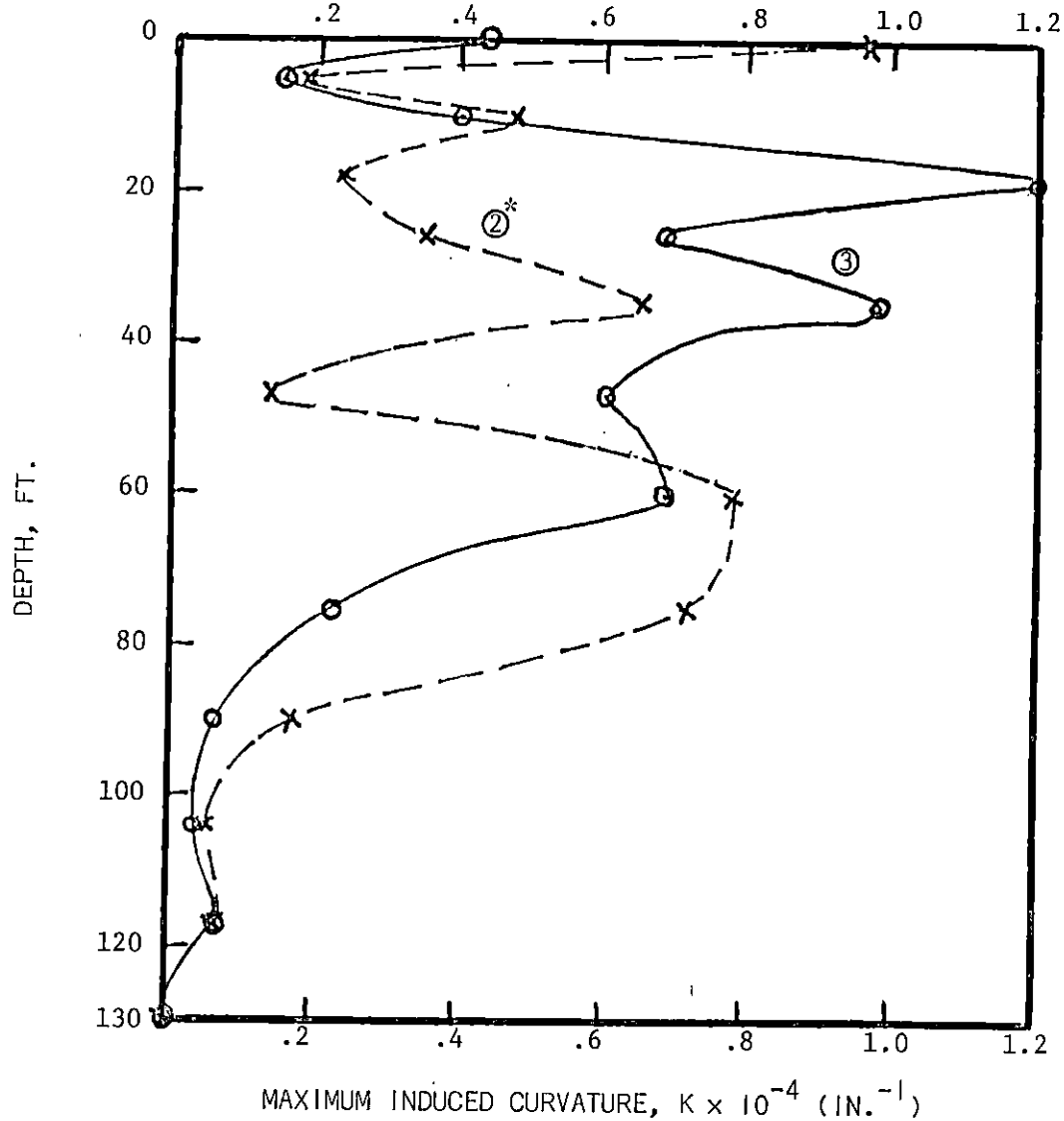

* Circled numbers within the graph denote the profile used for analysis

FIGURE 29: MAXIMUM INDUCED CURVATURES VS. DEPTH (TACOMA SITE; 14 IN. PILE SIZE; FIXED END CONDITION)

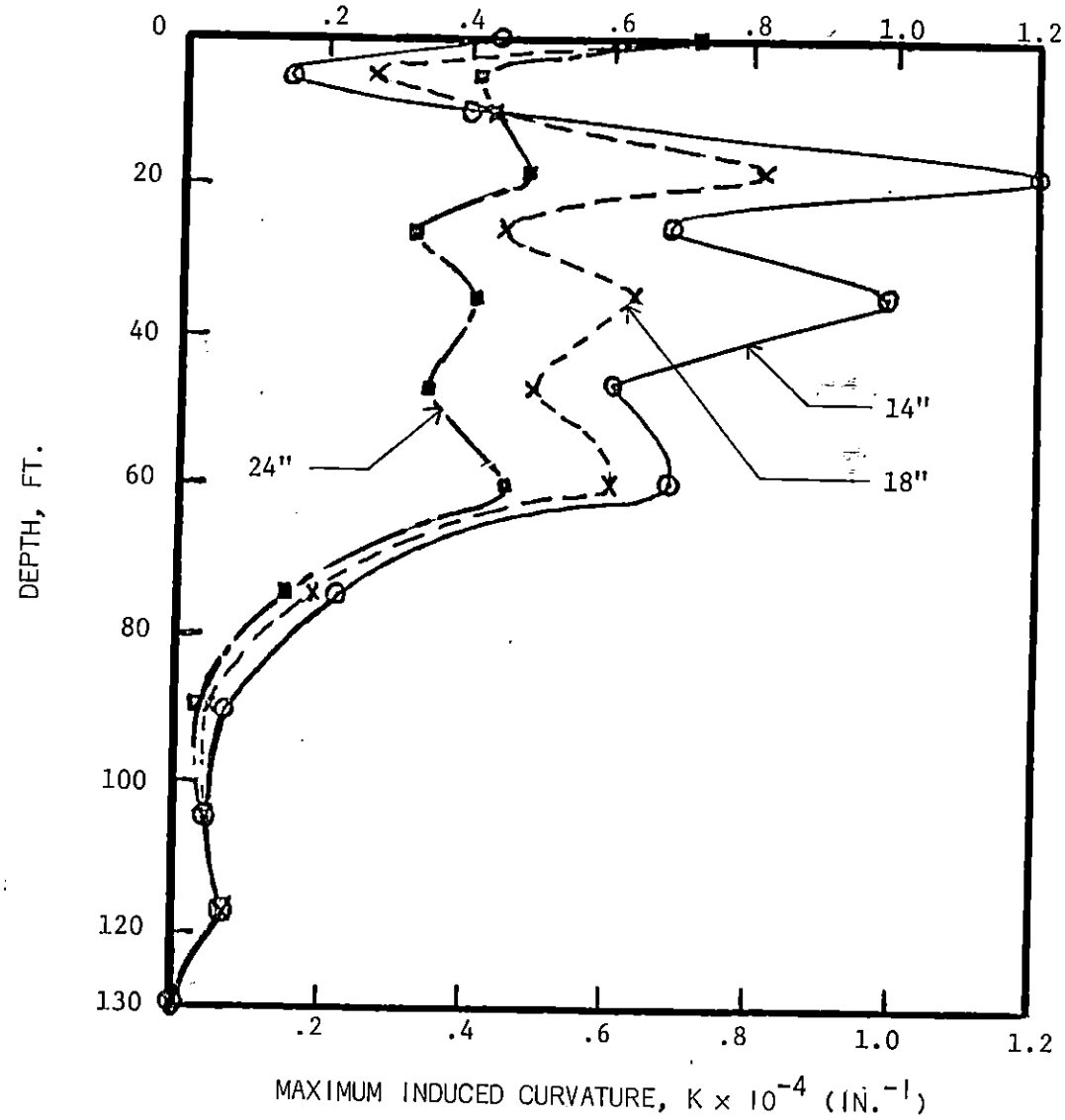

FIGURE 30: MAXIMUM INDUCED CURVATURES FOR DIFFERENT SIZE PILES (TACOMA SITE; 3RD PROFILE; FIXED END CONDITION)

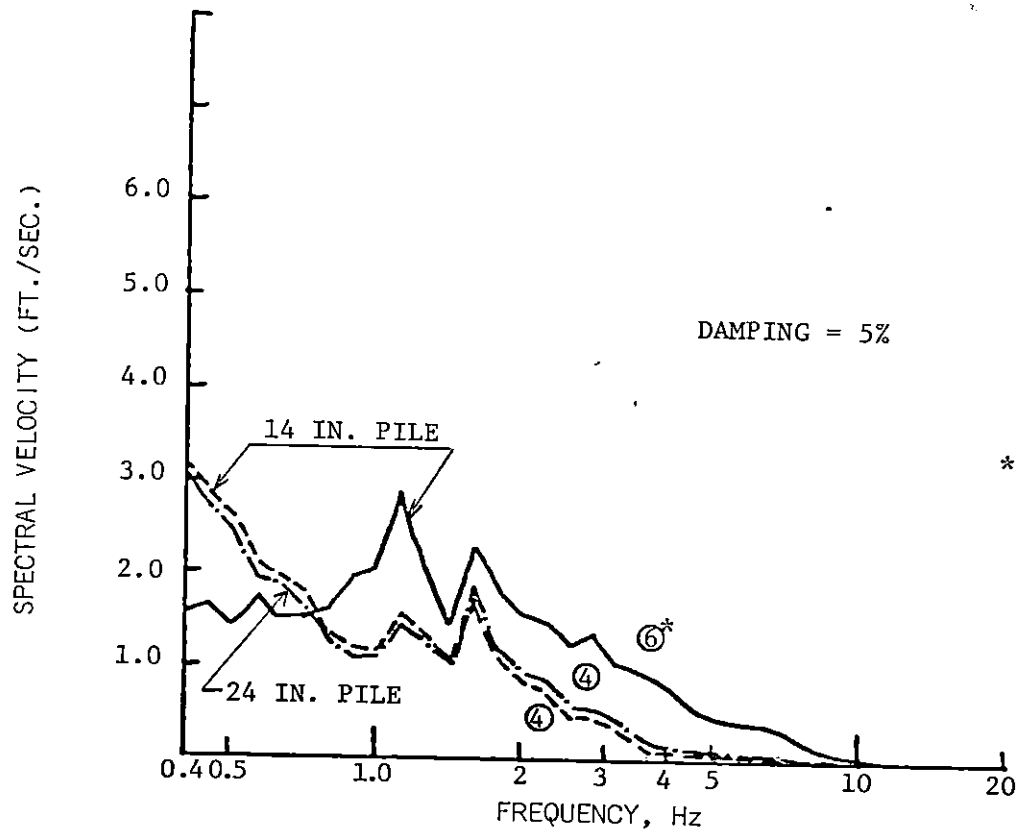

FIGURE 28: COMPARISON OF VELOCITY SPECTRA AT THE TOP OF PILE FOR THE TWO PROFILES (WEST SEATTLE SITE; FREE END CONDITION)

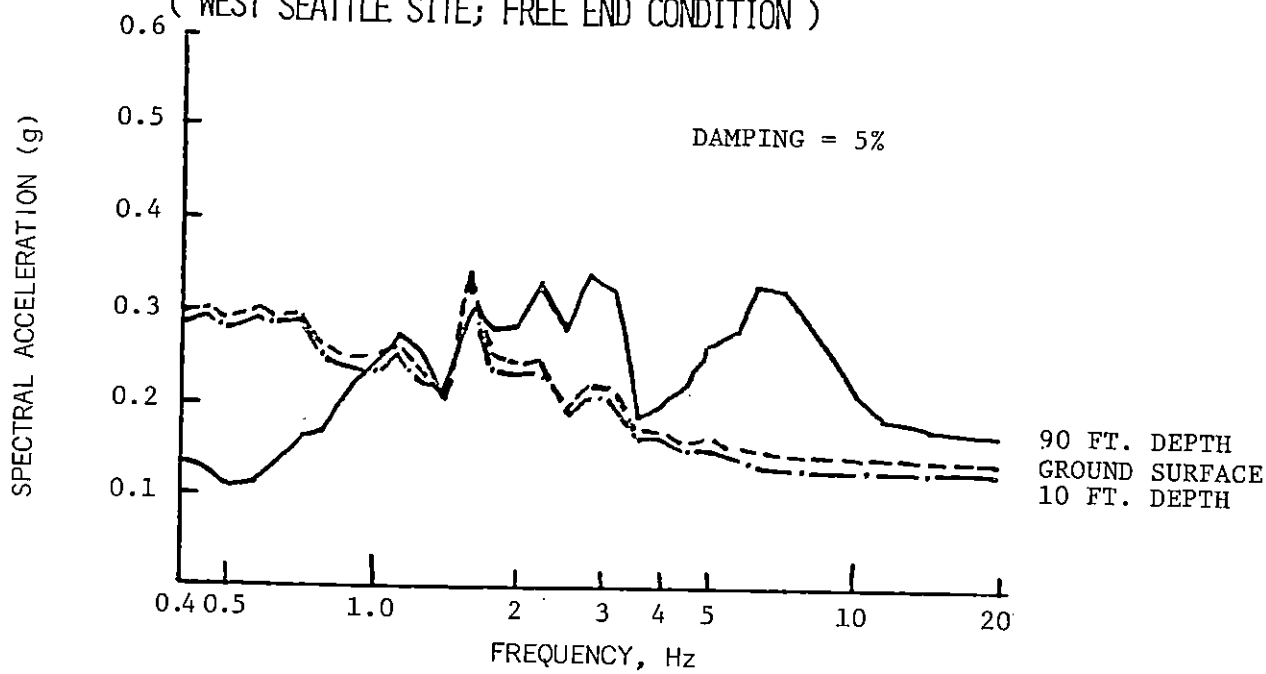

FIGURE 31: ACCELERATION SPECTRA AT VARIOUS DEPTHS ON THE PILE (TACOMA SITE; 14 IN. PILE)

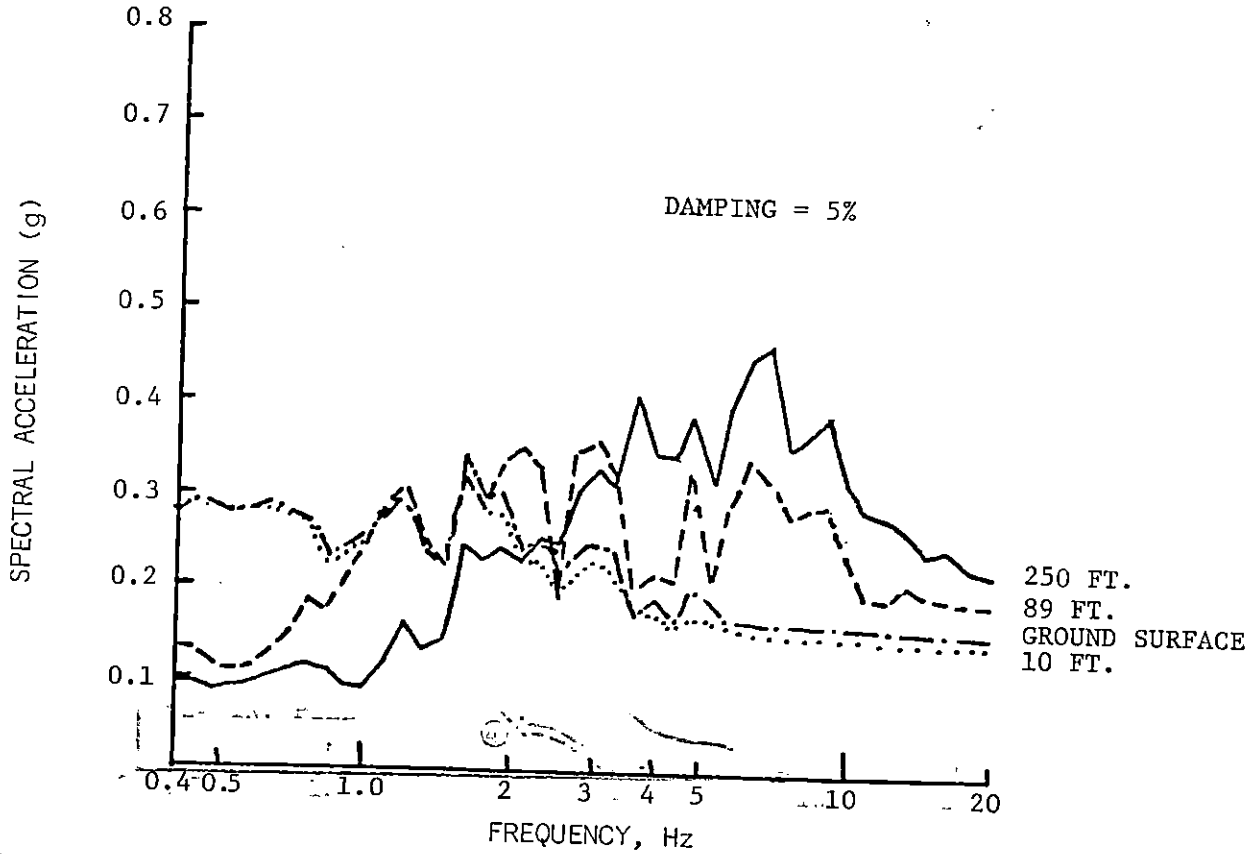

FIGURE 32: FREE-FIELD ACCELERATION SPECTRA AT DIFFERENT DEPTHS (TACOMA SITE; 3RD PROFILE)

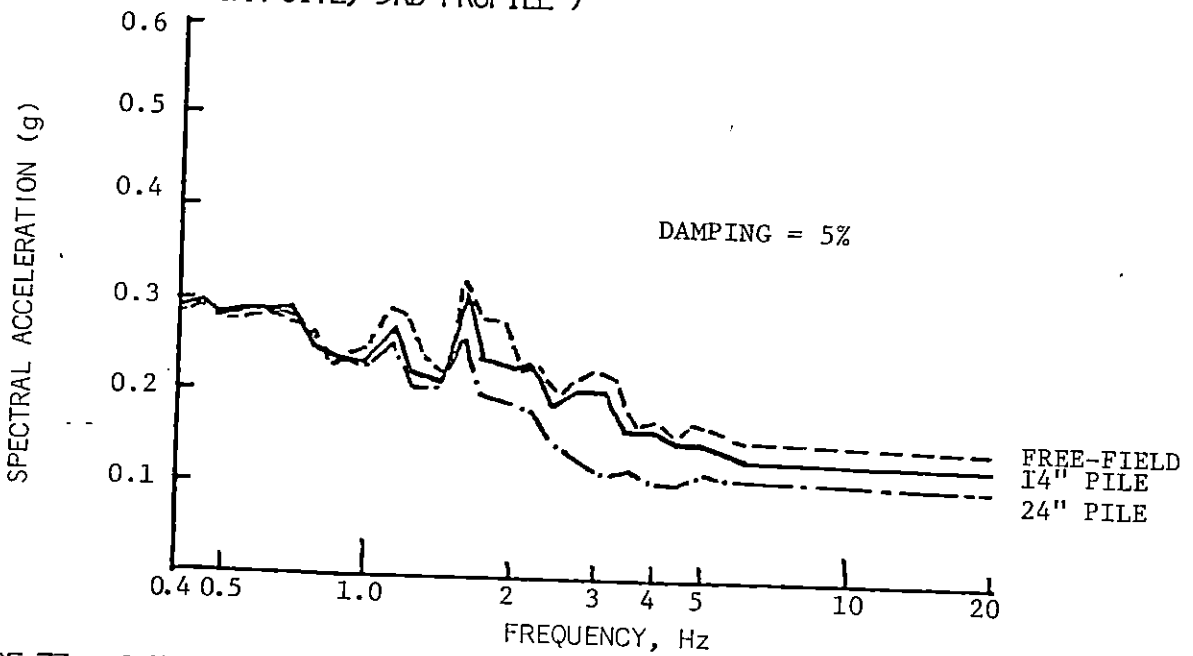

FIGURE 33: COMPARISON OF ACCELERATION SPECTRA AT A DEPTH OF 10 FT. ON THE PILE AND IN THE FREE-FIELD (TACOMA SITE; 3RD PROFILE)

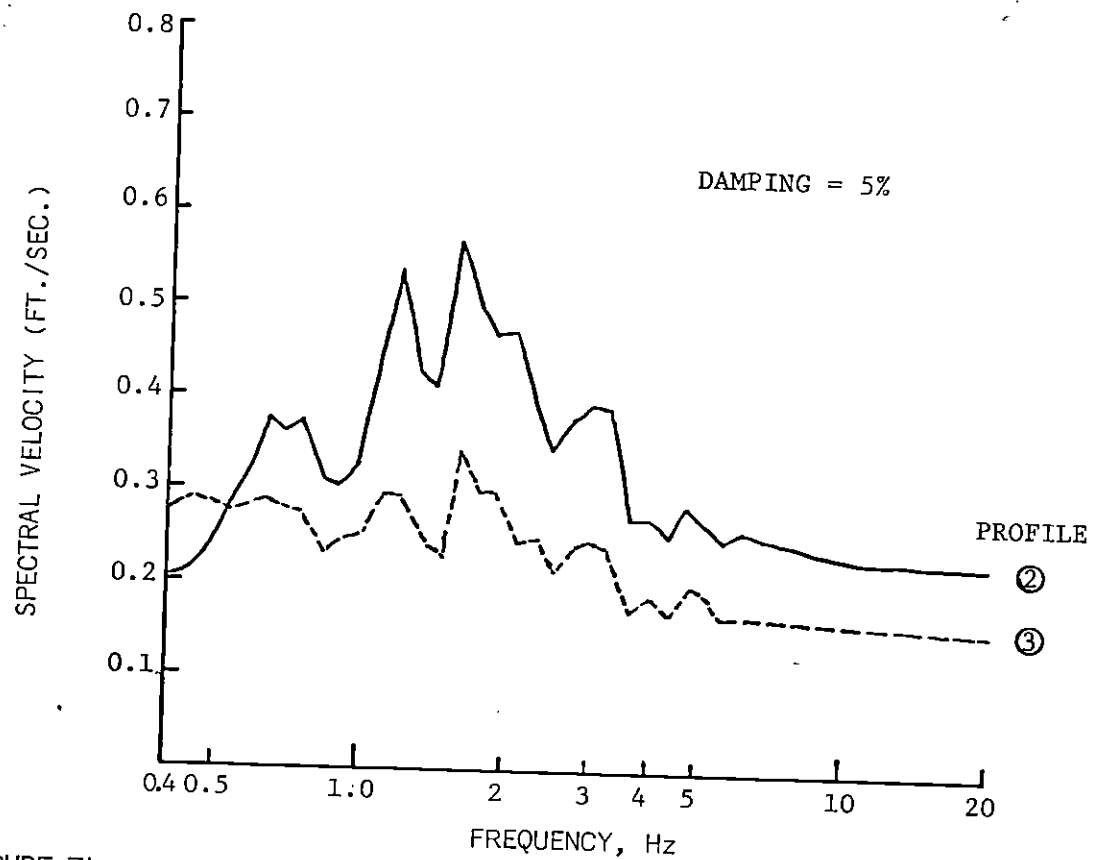

FIGURE 34: COMPARISON OF GROUND SURFACE ACCELERATION SPECTRA
(FOR THE TWO PROFILES AT TACOMA SITE)

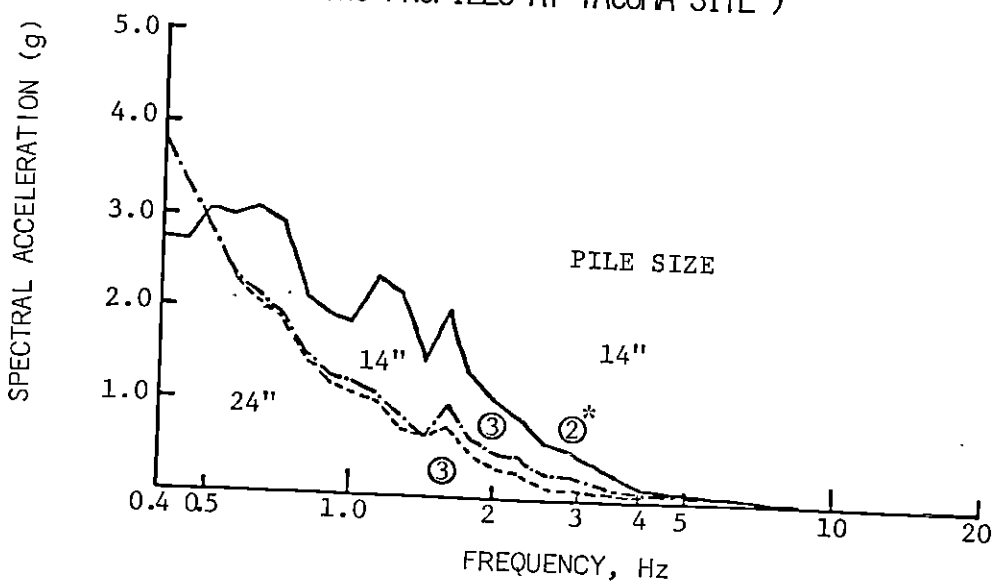

* Circled numbers within the graph denote the profile used for analysis

FIGURE 35: COMPARISON OF VELOCITY SPECTRA
(FOR THE TWO PROFILES AT TACOMA SITE; AT TOP OF PILE)

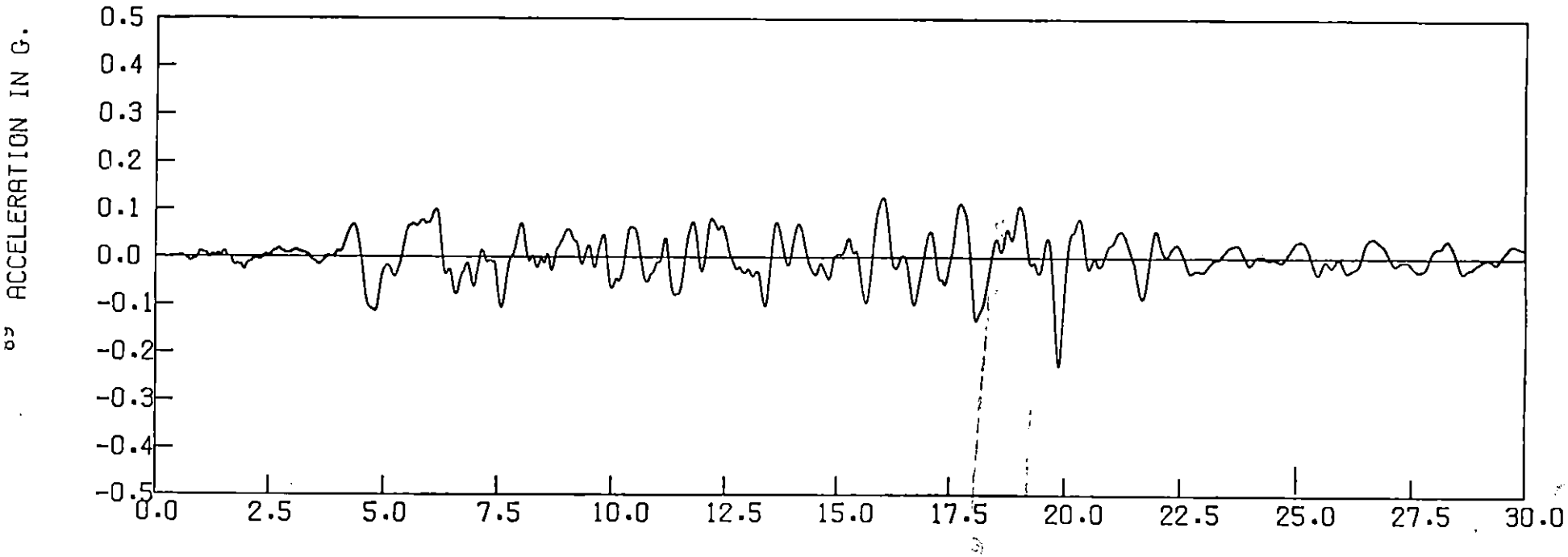

FIGURE 36: GROUND SURFACE MOTION (2ND PROFILE, TACOMA)

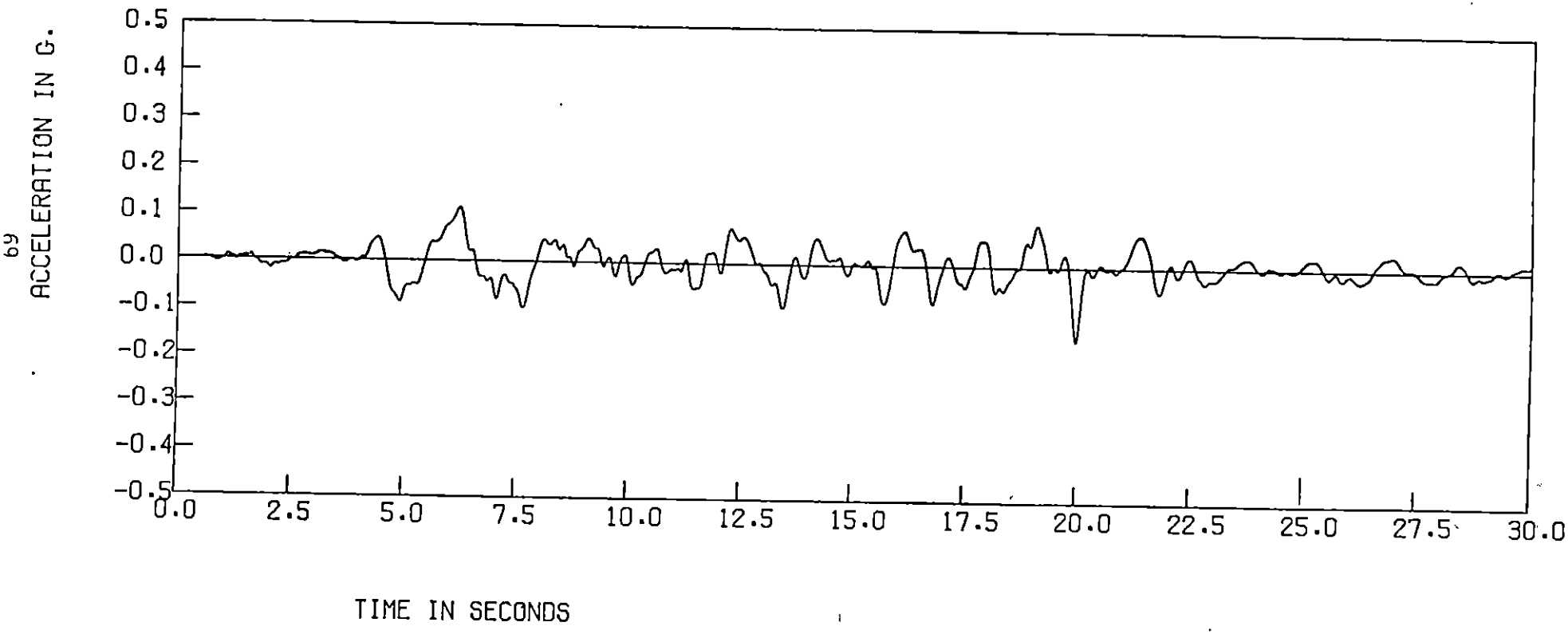

FIGURE 37: GROUND SURFACE MOTION (3RD PROFILE, TACOMA)

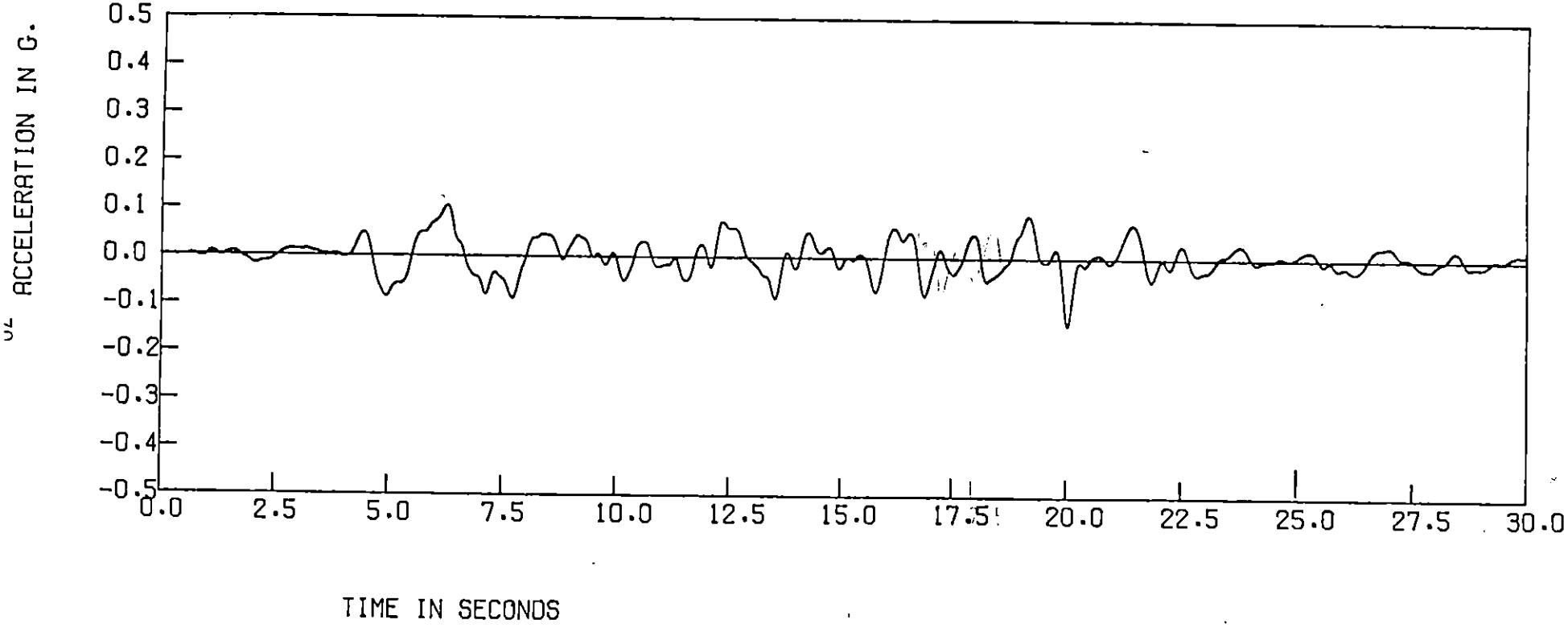

FIGURE 38: MOTION AT TOP OF 14 IN. PILE (3RD PROFILE, TACOMA)

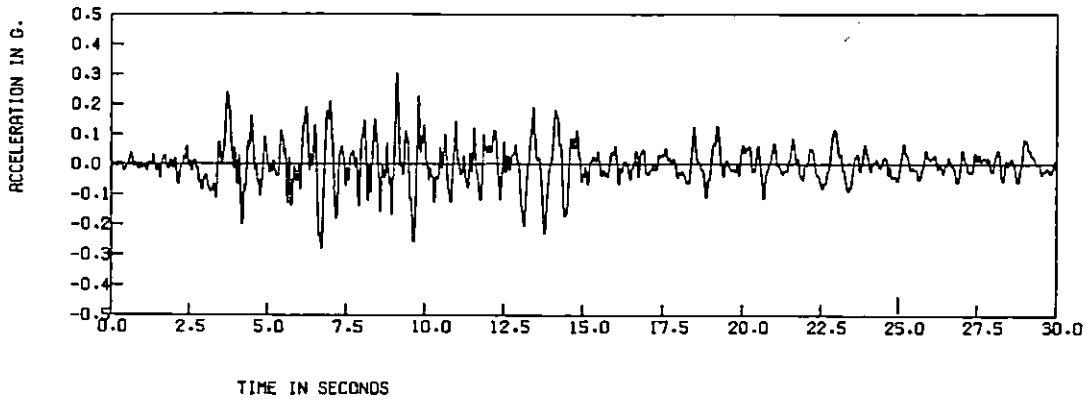

a) Base Rock Motion

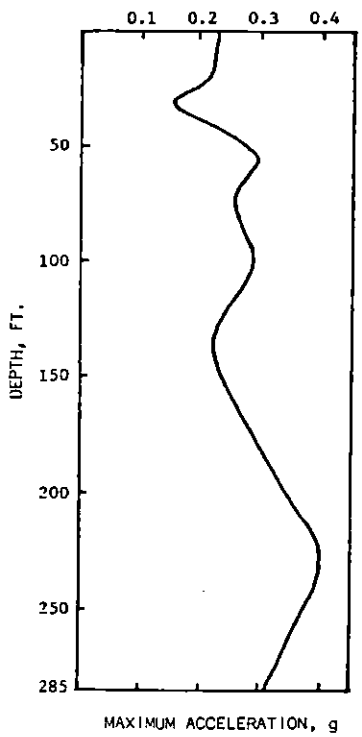

b) Free-Field Response

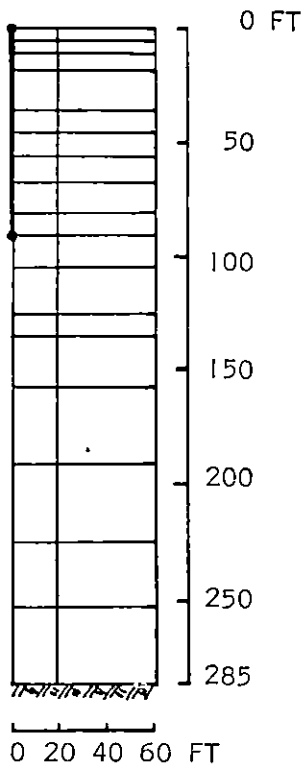

c) Finite Element Mesh

FIGURE 39: INPUT PARAMETERS FOR SOIL-PILE INTERACTION ANALYSES AT SAN FRANCISCO SITE

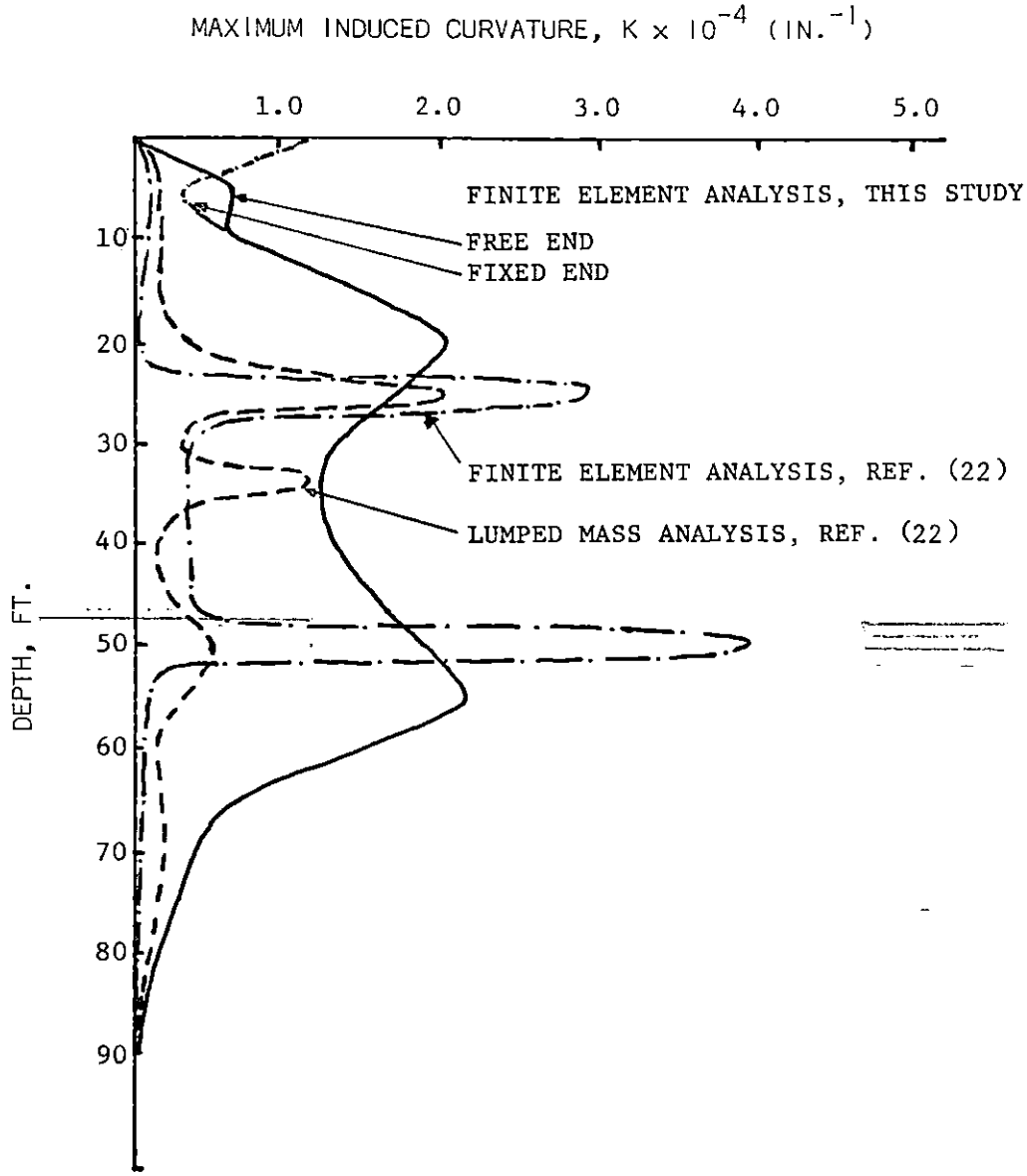

FIGURE 40: COMPARISON OF MAXIMUM PREDICTED CURVATURES FROM PRESENT AND PREVIOUS ANALYSES (12 IN. PILE)